EFFECTS OF THE RIBONUCLEASE INHIBITOR ON THE BIOLOGICAL ACTIVITY OF PANCREATIC-TYPE RIBONUCLEASES

by

Kimberly Anne Dickson

A dissertation submitted in partial fulfillment

of the requirements for the degree of

Doctor of Philosophy

(Biochemistry)

at the

UNIVERSITY OF WISCONSIN – MADISON

2006

A dissertation entitled

Effect of the Ribonuclease Inhibitor on the
Biological Activity of Pancreatic-Type Ribonucleases

submitted to the Graduate School of the
University of Wisconsin-Madison
in partial fulfillment of the requirements for the
degree of Doctor of Philosophy

by

Kimberly Anne Dickson

Date of Final Oral Examination: March 13, 2006

Month & Year Degree to be awarded: **December** **May** **August**

****

Approval Signatures of Dissertation Committee

Signature, Dean of Graduate School

Martin Cadwallader/EH

Committee's Page. This page is not to be hand-written except for the signatures

EFFECT OF THE RIBONUCLEASE INHIBITOR ON THE BIOLOGICAL ACTIVITY OF PANCREATIC-TYPE RIBONUCLEASES

Kimberly Anne Dickson

Under the supervision of Professor Ronald T. Raines

At the University of Wisconsin – Madison

The mammalian ribonuclease inhibitor (RI) is a 50-kDa cytosolic protein that binds to members of the bovine pancreatic ribonuclease (RNase A) superfamily with inhibition constants that range 10 orders of magnitude. Thus, RI plays an integral role in defining the biological activities of RNase A and its homologs. Onconase (ONC), an amphibian ribonuclease, does not bind to RI and is potently toxic to tumor cells. Conversely, RNase A and other mammalian homologs of RNase A bind to RI with femtomolar affinity and are rapidly inactivated upon entering a cell. Angiogenin, a human homolog of RNase A, possesses a nuclear localization signal and stimulates neovascularization. This dissertation describes the role of RI in the biological activities of pancreatic-type ribonucleases.

Variants of RNase A that evade RI can be toxic to tumor cells. The conformation stability of a ribonuclease also contributes to its cytotoxicity. We created A4C/K41R/G88R/V118C RNase A that reduced RI affinity (K41R/G88R) and increased the conformational stability (A4C/V118C). The variant was highly resistant to RI binding, but suffered a significant decrease in catalytic activity. The $(k_{cat}/K_m)_{cyto}$ value, which reports the ability of a ribonuclease to exert its ribonucleolytic activity in the presence of cytosolic RI, predicted that toxicity of A4C/K41R/G88R/V118C RNase A would not exceed its predecessors.

The complex formed by ANG and RI is amongst the tightest known in biology ($K_d \approx 1$ fM). ANG exerts its biological activity in the nucleus, whereas RI is present in the cytosol. We constructed G85R/G86R ANG that possessed 10^6-fold weaker affinity for RI but retained its catalytic activity. G85R/G86R ANG maintained its ability to translocate to the nucleus of HUVE cells and stimulated their migration at lower protein concentrations than did wild-type ANG. In addition, blood vessel growth stimulated by G85R/G86R ANG in rabbit cornea was more pronounced and more robust than with ANG. Thus, RI serves to regulate ANG-induced neovascularization.

Finally, we examined the effect of RI silencing on ribonuclease toxicity in human tumor cells using RNAi. Expression of an shRNA targeted to the RI gene resulted in a significant decrease in cytosolic RI levels. RI levels in some but not all tumor cell lines limited the cytotoxicity of ribonucleases. We conclude that the salient features of the mechanism of ribonuclease cytotoxicity remain to be discovered.

Acknowledgements

I am grateful to many people for the support and assistance that they have offered me during my graduate career. First, I would like to thank my advisor, Ron Raines, who has provided a vital mix of encouragement, enthusiasm, creativity, and resources with which to conduct this research. The Raines lab has fostered my intellectual development and helped me realize my career goals.

Many members of the Raines lab, past and present, have contributed greatly to this work. Pete Leland, Marcia Haigis, and Tony Klink introduced me to many aspects of ribonuclease biochemistry and have been invaluable resources long after their tenure at UW–Madison. I would like to thank the chemists of the Raines lab, especially Sunil Chandran, for the opportunities to collaborate on a variety of projects. While they are not part of this dissertation, those endeavors have greatly expanded my knowledge of chemistry and my perspectives as a scientist. My classmate, Steve Fuchs, and the "younger" members of the Raines lab have all provided valuable advice and support over the years. In particular, I would like to thank Rebecca Turcotte and Jeremey Johnson, with whom I shared many fascinating discussions, scientific and otherwise.

I am also very grateful to the members of my thesis committee, who have supported my research for the past six years and continue to support me as I launch my career at Macalester College. Their wisdom and thoughtful advice is greatly appreciated.

Finally, I would like to thank my family for their endless support and encouragement. My graduate career has been long and sometimes difficult. Nevertheless, my parents and my

husband, Jeff, have offered consistent encouragement and support. This dissertation would have never been possible without their love.

Table of Contents

List of Tables

List of Figures

List of Abbreviations

ANG.....human angiogenin

BS-RNase.....bovine seminal ribonuclease

DEPC.....diethylpyrocarbonate

DTT.....dithiolthreitol

EDTA.....ethylenediaminetetraacetic acid

IPTG.....isopropyl-1-thio- -D-galactopyranoside

MES.....2-[N-morpholino)ethanesuphonic acid

ONC.....onconase

PBS.....phosphate-buffered saline

RI.....ribonuclease inhibitor

RNAi.....RNA inhibition

RNase .....human pancreatic ribonuclease

RNase A.....bovine pancreatic ribonuclease

shRNA.....short hairpin RNA

SDS-PAGE.....sodium dodecyl sulfate–polyacrylamide gel electrophoresis

Tris.....tris(hydroxymethyl)aminomethane

T_m.....midpoint of the thermal denaturation curve

UV.....ultraviolet

6-FAM.....6-carboxyfluorescein

6-TAMRA.....6-carboxytetramethylaminorhodamine

Chapter One

Introduction

Portions of this chapter were published as:

Dickson, K. A., Haigis, M. C., and Raines, R. T. (2005). Ribonuclease Inhibitor: Structure and Function. *Progress in Nucleic Acid Research and Molecular Biology*. **80**, 349-374.

The mammalian ribonuclease inhibitor (RI) is a 50-kDa cytosolic protein that binds to pancreatic-type ribonucleases with femtomolar affinity and renders them inactive (for other reviews, see (Roth 1967; Blackburn and Moore 1982; Lee and Vallee 1993; Hofsteenge 1997; Shapiro 2001). Complexes formed by RI and its target ribonucleases are among the tightest of known biomolecular interactions. The three-dimensional structure of RI is likewise remarkable, being characterized by alternating units of α-helix and β-strand that form a striking horseshoe shape (Fig. 1A) (Kobe and Deisenhofer 1993). The repeating structural units of RI possess a highly repetitive amino acid sequence that is rich in leucine residues (Hofsteenge *et al.* 1988; Lee *et al.* 1988). These leucine-rich repeats (LRRs) are present in a large family of proteins that are distinguished by their display of vast surface areas to foster protein–protein interactions (Janin 1994; Kobe and Deisenhofer 1994; Shapiro *et al.* 1995; Kobe and Kajava 2001). The unique structure and function of RI have resulted in its emergence as the central protein in the study of LRRs, as well as its widespread use as a laboratory reagent to eliminate ribonucleolytic activity (Pasloske 2001).

The biological role of RI is not known in its entirety. The ribonucleases recognized by RI are secreted proteins, whereas RI resides exclusively in the cytosol. Nevertheless, RI affinity has been shown to be the primary determinant of ribonuclease cytotoxicity: only ribonucleases that evade RI can kill a cell (for reviews, see (Youle and D'Alessio 1997; Leland and Raines 2001; Matousek 2001; Makarov and Ilinskaya 2003). In addition, the complex of RI with human angiogenin (ANG), which stimulates neovascularization by activating transcription in the nucleus (Moroianu and Riordan 1994; Xu *et al.* 2002), is the tightest of known RI·ribonuclease complexes. Yet, a role for RI in angiogenesis is not clear. Also intriguing are the 30–32 cysteine residues of RI, all of which must remain reduced for

the protein to retain activity (Fominaya and Hofsteenge 1992). These observations have lead researchers to hypothesize multiple biological roles for RI: (1) to protect cells from invading ribonucleases, (2) to regulate or terminate the activity of ribonucleases with known intracellular functions, and (3) to monitor the oxidation state of the cell in response to factors such as aging and oxidative stress. Here, we review the salient features of RI biochemistry and structure and thereby provide a context for examining the roles of RI in biology.

Biochemical Properties

The inhibitory activity of RI in guinea pig liver extracts was discovered in 1952 (Pirotte and Desreux 1952). This activity was inactivated by proteases, heat, or sulfhydryl-group modification, and was sensitive to changes in pH (for a review, see (Roth 1962). In addition, the inhibitory activity was isolated in the supernatant fraction during a high-speed centrifugation, indicative of cytoplasmic localization. In the 1970's, techniques were developed to purify RI to homogeneity, enabling its biochemical characterization (Blackburn *et al.* 1977; Blackburn and Moore 1982). Since then, RI has been isolated from numerous mammalian sources, including brain (Burton *et al.* 1980; Cho and Joshi 1989) (Nadano, 1994), liver (Nadano, 1994; Gribnau *et al.* 1970; Burton and Fucci 1982), testis (Ferreras *et al.* 1995), and erythrocytes (Moenner *et al.* 1998).

Purification. RI is particularly abundant in mammalian placenta and liver, which have served as the major source of RI for purification. Human placental RI was first purified to homogeneity using a combination of ion-exchange and ribonuclease-affinity chromatography (Blackburn *et al.* 1977). The tight complex formed by RI and bovine pancreatic ribonuclease (RNase A (Raines 1998); EC 3.1.27.5) has been exploited to achieve a $>10^3$-fold purification

of RI in a single chromatographic step using immobilized RNase A. Today, most purification methods rely upon such ribonuclease-affinity chromatography, followed by anion-exchange chromatography (Garcia and Klebe 1997). Using these purification techniques, approximately 6 mg RI per kg of wet tissue has been isolated from mammalian liver (Burton and Fucci 1982) and placenta (Blackburn 1979). Human erythrocytes are also rich in RI—the erythrocyte fraction of 100 mL of blood has yielded 430 μg of RI (Moenner *et al.* 1998).

Several recombinant systems for the production of RI have been reported, three from Escherichia coli and one from Saccharomyces cerevisiae (Vescia *et al.* 1980; Lee and Vallee 1989; Vicentini *et al.* 1990). Low yields and insolubility have proven to be recurring problems in producing recombinant RI. To date, the most efficient recombinant system utilizes the trp promoter from E. coli to drive expression of porcine RI, and yields approximately 10 mg of RI per liter of culture (Klink *et al.* 2001).

Characterization. RI is an acidic (pI 4.7) cytosolic protein that binds to pancreatic-type ribonucleases with 1:1 stiochiometry (Blackburn and Jailkhan 1979). Members of the RNase A superfamily of proteins that are inhibited by RI include RNase A, human pancreatic ribonuclease (RNase 1), ANG, eosinophil-derived neurotoxin (EDN, also known as RNase 2), RNase 4, and monomers of bovine seminal ribonuclease (BS-RNase). When complexed with RI, these ribonucleases are no longer able to bind or degrade RNA (Lee and Vallee 1993). RI is ineffective against known non-mammalian homologs of RNase A. The amino acid sequences of human, porcine, mouse, and rat RI share 66% identity (Fig. 2) (Hofsteenge *et al.* 1988; Lee *et al.* 1988; Kawanomoto *et al.* 1992; Haigis *et al.* 2002). One third of the residues that differ are conservative substitutions. To date, RI from human and pigs have

been characterized most thoroughly and exhibit many identical properties (for reviews, see (Hofsteenge 1997; Shapiro 2001). Thus, the source of RI will be discussed herein only if a significant divergence occurs with respect to a particular experimental observation.

The affinity of RI for ribonucleases is extraordinary. Accordingly, substantial effort has been invested in characterizing RI–ribonuclease interactions (for a review, see (Shapiro 2001). Techniques to assess binding rely upon the imposition of physical changes or inhibition of catalytic activity. A purely physical method is more convenient to use for ribonucleases with low catalytic activity, such as ANG (Lee *et al.* 1989). For example, stopped-flow techniques and the 50% increase in the fluorescence of Trp89 of ANG upon binding to RI have been used to study the association of RI with ANG. They report a two-step binding mechanism that involves formation of a loose enzyme·inhibitor complex (E·I) followed by isomerization to form a tight complex (E·I*), as in Eq. (1):

$$E+I \underset{k_{-1}}{\overset{k_1}{\rightleftharpoons}} EI \underset{k_{-2}}{\overset{k_2}{\rightleftharpoons}} EI^* \qquad (1)$$

ANG and RI rapidly form a loose complex ($K_1 = k_{-1}/k_1 = 0.53\ \mu M$), which converts slowly ($k_2 = 97\ s^{-1}$) to a stable complex. The association rate constant, $k_a = k_1k_2/(k_{-1} + k_2)$ was found to be $1.8 \times 10^8\ M^{-1}s^{-1}$. The dissociation rate constant, $k_d = k_{-1}k_{-2}/(k_{-1}+ k_2)$, was measured by the monitoring release of ANG from the RI·ANG complex in the presence of excess RNase A as a scavenger, and found to be $1.3 \times 10^{-7}\ s^{-1}$ (Lee and Vallee 1989). This value corresponds to a half-life of 62 days for the RI·ANG complex. The resulting value of the equilibrium dissociation constant, $K_d = k_d/k_a = 7.1 \times 10^{-16}$ M, is exceptionally low, and comparable to the $K_d = 6 \times 10^{-16}$ M of the avidin·biotin complex (Green 1975). A competition assay based on

fluorescence changes in ANG has been used to measure $K_d = 4.4 \times 10^{-14}$ M for the RI·RNase A complex (Lee *et al.* 1989).

RI has only a slight effect on the fluorescence of RNase A, which lacks tryptophan residues. Enzymatic assays in which the value of K_i is determined by the ability of RI to compete with RNA are viable alternatives for this and other ribonucleases that possess high catalytic activity. In general, enzymatic assays require that ribonucleolytic activity can be performed at low enzyme concentrations—no more than 2 orders-of-magnitude greater than the K_i (Vicentini *et al.* 1990). Enzymological methods have been used to assess the affinity of RI for RNase A, RNase 1, and RNase 4 (Table I) (Vicentini *et al.* 1990; Zelenko *et al.* 1994; Boix *et al.* 1996; Hofsteenge *et al.* 1998). For examples, the values of $k_a = 1.7 \times 10^8$ $M^{-1}s^{-1}$, $k_d = 9.8 \times 10^{-6}$ s^{-1}, and $K_i = 5.9 \times 10^{-14}$ M were determined by measuring the decrease in ribonucleolytic activity upon addition of RI.

The affinity of RNase A and RNase 2 for RI has also been assessed with a combination of physical and enzymological techniques. The k_d value for the RI·RNase A complex was determined by measuring the release of RNase A in the presence of ANG as a scavenger (Lee *et al.* 1989; Lee *et al.* 1989). The concentration of free RNase A was detected by high-performance liquid chromatography or by enzymatic activity with RNA substrates that are not cleaved by ANG. Similar assays have been used to determine the kinetic parameters for the RI·RNase 2 interaction (Shapiro and Vallee 1991). The kinetic and thermodynamic parameters determined with a variety of physical and enzymatic methods are in gratifying agreement (Table I).

A fluorescence-based assay has been developed to facilitate rapid measurement of K_d for a wide variety of RI·ribonuclease complexes (Abel *et al.* 2001). This assay employs

fluorescein-labeled G88R RNase A, which has diminished affinity for RI and exhibits an approximately 20% decrease in fluorescence when bound to RI. Titration of RI with fluorescein-G88R RNase A yielded $K_d = 0.55 \times 10^{-9}$ M for the complex. A competition assay using fluorescein-G88R RNase A was then used to determine the K_d value of unlabeled ribonucleases (Table II). This assay is limited to measuring complexes with K_d values in the nanomolar range or higher, as tighter complexes take too long to reach equilibrium. Nonetheless, this assay has proven to be valuable for determining K_d values of numerous RNase A variants, some of which possess low catalytic activity (Haigis *et al.* 2002; Dickson *et al.* 2003).

Structure

Three-Dimensional Structure. Leucine is the most abundant residue in RI, comprising 18% of its amino acids (Blackburn *et al.* 1977; Burton and Fucci 1982). In 1988, the amino acid sequence of RI from both porcine liver and human placenta was elucidated, revealing that RI is comprised entirely of leucine-rich repeats (LRR) (Hofsteenge *et al.* 1988; Lee *et al.* 1988). Two types of alternating repeats have been described, A-type (which contains 28 residues) and B-type (which contains 29 residues). Porcine RI is built from 8 A-type and 7 B-type repeats, flanked by short terminal segments (Fig. 2) (Kobe and Deisenhofer 1994).

RI was the first LRR protein to be crystallized and have its three-dimensional structure determined by X-ray diffraction analysis (Kobe and Deisenhofer 1993). Its horseshoe shape is one of the most captivating of protein structures. The alternating A- and B-type LRR motifs correspond to structural units, each consisting of an α-helix and β-strand connected by loops (Fig. 2A and 2B). The symmetric and non-globular arrangement of LRRs

represents a new protein fold (for reviews, see: (Kobe and Deisenhofer 1995; Kajava 1998; Kobe and Kajava 2001). The LRR units of RI are arranged so that the α-helices and β-strands are aligned parallel to a common axis (Fig. 1A). An extended β-sheet defines the inner circumference of the horseshoe and provides a vast surface for interacting with other proteins. Leucines and other aliphatic residues are essential components of the hydrophobic core of the protein, and serve to stabilize the interactions βween the LRR units (Fig. 3). The curvature of the RI horseshoe is determined by the difference in distance βween neighboring β-strands and α-helices (Kajava 1998; Kobe and Kajava 2001). The curvature of RI is quite pronounced, as the addition of only 5 more LRR units to the native 15 would cause the termini of RI to collide (Kobe and Deisenhofer 1993).

A Model Leucine-Rich Repeat Protein. The LRR was first described with respect to the leucine-rich α2-glycoprotein found in human serum (Takahashi *et al.* 1985). RI was the first cytosolic protein discovered to possess LRRs (Hofsteenge *et al.* 1988; Lee *et al.* 1988). In the past decade, more than a hundred LRR proteins have been identified; these proteins have been found to perform remarkably different functions. In most LRR proteins, however, the LRRs appear to serve as the interface for a protein–protein interaction (for reviews, see (Kobe and Deisenhofer 1995; Kajava 1998).

LRR proteins have been classified into subfamilies base on the organism of origin, cellular localization, and LRR consensus sequence (Kobe and Kajava 2001). To date, seven LRR subfamilies of proteins have been described (Table III), and additional subfamilies could arise with the discovery of more LRR proteins. Members of the RI-like subfamily are intracellular proteins found in animals, and are characterized by repeats of 28/29 amino acids that possess the sequence LXXLXLXX(N/C)XL. Other members of the RI-like subfamily

include human MHC class II transactivator (P33076), Ran GTPase activating protein from Saccharomyces pombe (P46060), RNA1 gene product from Saccharomyces cerevisiae (X17376), and the mouse homolog of RNA1 (U20857).

In general, the β-strand region of the repeat is the most conserved among LRR proteins (Kobe and Kajava 2001). Subfamilies differ primarily in the secondary structure displayed in the regions βween the β-strands (Table III, Fig. 4) (Kobe and Kajava 2001). Short LRR units result in extended conformations in the interstrand region. For example, members of the bacterial subfamily of LRR proteins are built from repeating units of only 20 amino acid residues. In the SDS22-like family, the α-helix found in RI-like proteins is often replaced by a 3_{10} helix (Price *et al.* 1998). In the structure of YopM, an extracellular protein that confers bacteria with virulence, the α-helix is replaced with a polyproline type-II (PII) helix (Table III) (Evdokimov *et al.* 2001). Structures of representative proteins from five subfamilies illustrate the diversity in the size and shape of LRR proteins (Fig. 4) (Schulman *et al.* 2000; Matteo *et al.* 2003; Schott *et al.* 2004).

The structure of RI is repetitive and symmetrical, and its surface area is vast and largely concave (Fig. 1A). These unusual attributes make RI a potential platform for the creation of new receptors. Towards this goal, a consensus LRR domain determined from the sequences of rat, pig, and human RI has been used to generate proteins containing 2–12 LRRs (Stumpp *et al.* 2003). Biophysical analyses of the RI-like proteins showed monomeric behavior and circular dichroism spectra characteristic of wild-type RI, suggesting that RI-like proteins are viable templates for engineering.

Gene Structure and Evolution. RI homologs have been identified in numerous mammalian species and have been found in nearly every type of organ, tissue, and gland

investigated to date. Only one copy of the RI gene exists in the human genome (Crawford *et al.* 1989), and RIs isolated from different tissues of the same species typically have the same amino acid sequence. Still, subtle divergences exist. For example, alternative splice-site forms have been identified in the 5' untranslated region of RI from human placenta (Crawford *et al.* 1989). Yet, Northern blot analysis of RI from both placenta and HeLa cells indicate that RI is expressed as a single transcript (Lee *et al.* 1988; Schneider *et al.* 1988).

Proteins from all LRR subfamilies are capable of forming horseshoe-like structures similar to that of RI (Fig. 4) (Kobe and Kajava 2001). Modeling studies suggest that the characteristic LRR of a given LRR subfamily cannot be replaced with the LRR from another subfamily (Kajava and Kobe 2002). Despite similar tertiary structures, the interstrand segments of LRR proteins exhibit markedly different packing interactions, which are not compatible. These observations suggest that the LRRs from different subfamilies have evolved independently, rather than from a single ancestor.

The human RI gene evolved via gene duplication (Haigis *et al.* 2002). Structural analysis of the RI gene reveals that the exons of RI correspond directly with the LRR units of RI: each exon codes for two segments of α-helix and β-strand (Fig. 1A). In addition, the exons are exactly the same length (171 bases) and exhibit a high degree of identity (50–60% for the 7 internal exons). Apparently, each module of RI arose from a gene duplication event. Not all of the modules of RI are necessary for RI to bind RNase A (Lee and Vallee 1990; Hofsteenge *et al.* 1991). In fact, as many as two internal modules (113 residues) of RI can be deleted without abolishing its ability to bind to RNase A or inhibiting its catalytic activity (Lee and Vallee 1990). Expansion of the RI gene (and protein) to its current size could have facilitated recognition of additional ribonucleases.

The duplication of RI exons occurred rapidly, perhaps in response to the evolution and divergence of members of the RNase A superfamily (Haigis *et al.* 2002). The RI gene has continued to diverge slowly over a long period of time. Although there is no direct evidence to support positive selection in the evolution of RI exons, it is probable that RI has co-evolved with its complementary ribonucleases. The binding of RI to members of the RNase A superfamily is class specific. For example, human RI will bind to mammalian ribonucleases, but will not inhibit homologous ribonucleases isolated from chicken liver or frog oocytes (Roth 1962; Kraft and Shortman 1970), consistent with distinct pathways of co-evolution.

Complexes with Ribonucleases

Three-Dimensional Structures. The three-dimensional structures of porcine RI (Kobe and Deisenhofer 1993) and the porcine RI·RNase A complex (Kobe and Deisenhofer 1995) were determined in 1993 and 1995 (Fig. 1B). Approximately 2900 $Å^2$ of surface area is buried at the RI–RNase A interface, which is 60% more than in a typical antibody·antigen complex (Kobe and Deisenhofer 1995). The extensive buried surface likely accounts for its exceptionally high affinity for ribonucleases, producing complexes with a K_d value that is 10^3-fold lower than that of a typical antibody·antigen complex. The RI–RNase A interaction appears to rely on Coulombic forces more than do most protein–protein interactions. The β-sheet lining the inner circumference of the horseshoe contributes only 9 of the residues involved in complex formation. Two contact residues are found in α-helical regions of RI, and the remaining 17 contacts are found in loops connecting the C-termini of the β-strands

with the N-termini of the α-helices. Upon binding to RNase A, the structure of RI flexes uniformly, and the distance βween the N- and C-termini of RI increases by more than 2 Å.

RNase A is a kidney-shaped molecule (Wlodawer 1985). The active site of the enzyme is located in a cleft βween two lobes of the protein. RI inhibits RNase A by blocking the active site; many of the amino acid residues of RNase A that are important for RNA binding and catalysis also interact with RI (Kobe and Deisenhofer 1996). Few of the contacts provided by RI mimic the RNase A–RNA interaction, though the phenolic ring of Tyr433 does lie in a nucleoside binding site. Thirteen separate patches of residues (28 amino acids) from dispersed regions of RI interact with 3 clusters of residues (24 amino acids) from RNase A. The C-terminal module of RI forms extensive contacts with RNase A, accounting for approximately 30% of the contacts βween the two proteins.

The three-dimensional structure of the human RI·ANG complex was determined in 1997 (Papageorgiou *et al.* 1997). Although the overall docking of ANG with RI is similar to that of RNase A (Fig. 1C), the flexing of RI in the RI·RNase A complex is not apparent in the RI·ANG complex. As in the RI·RNase A complex, the active site of ANG is blocked by numerous contacts with the C-terminus of RI (Papageorgiou *et al.* 1997). Yet, both substantial and subtle differences are evident in the two complexes. For example, Lys320 of human RI contacts Asp41 of ANG, whereas the analogous residue in porcine RI, Lys316, interacts with Glu86 of RNase A. Using site-directed mutagenesis, the phenyl group of Tyr434 has been shown to interact with both ANG and RNase A (Chen and Shapiro 1999). Conversely, the phenolic hydroxyl group of Tyr437 interacts with RNase A, whereas the phenyl group of that residue contacts ANG. The dissimilar binding interactions of the two

complexes indicate that the broad specificity of RI for pancreatic-type ribonucleases is derived from a remarkable ability to recognize specific features of each ribonuclease.

Biomolecular Analyses. The amino acid sequences of RI vary only slightly βween species. Yet, the ribonucleases they inhibit differ significantly, possessing as little as 30% amino acid sequence identity. In addition, the ribonucleases that form tight complexes with RI do not exhibit markedly increased sequence identity with each other than with homologous ribonucleases that do not bind to RI.

Prior to the elucidation of its three-dimensional structure, truncated variants of RI were constructed to examine the requirements of RI binding (Lee and Vallee 1990; Hofsteenge *et al.* 1991). For example, a library of RI variants was constructed by the deletion of one or more LRR modules (one A-type repeat and one B-type repeat) (Lee and Vallee 1990). RI variants missing either modules 3 and 4 or module 6 were found to retain affinity for RNase A, whereas deletion of other modules disrupted binding completely. In addition, deletion of module 6 had a substantially greater effect on the affinity of RI for ANG than for RNase A. In another example, RNase A was found to bind to Δ1–90 RI with only a twofold increase in the value of K_i (Hofsteenge *et al.* 1991). These data provided the first evidence of the modular structure of RI and demonstrated that RI uses disparate regions of its massive surface area to bind to ribonucleases.

The structure of crystalline RI·RNase A shows Gly88 of RNase A in a hydrophobic pocket formed by three tryptophan residues of RI. To generate an RI-evasive variant of RNase A, Gly88 was replaced with an arginine residue (Leland *et al.* 1998). The steric bulk of arginine hinders RI binding, and this single substitution increases the K_i value by 10^4-fold. A pocket can be created in RI to relieve the steric strain in the RI·RNase A complex imposed

by an arginine residue at position 88 of RNase A. Replacing Trp264 in RI with an alanine residue allows RI to accommodate Arg88 of G88R RNase A. Although wild-type RI and the W264A variant inhibit RNase A to a similar extent, only the variant protects 16S- and 23S-rRNA from degradation by G88R RNase A. These data demonstrated that the "knobs-into-holes" concept (Crick 1952) is applicable to an RI·ribonuclease complex.

Mutagenesis of key binding residues of RI was found to have varying effects on binding energy. Replacing some residues that appear to contact RNase A closely (e.g., Glu287, Lys320, Glu401, or Arg457) had little effect on binding (Chen and Shapiro 1997). On the other hand, Tyr434, Asp435, Tyr437, and Ser460 of RI were found to constitute a "hot spot" of binding energy. Only one of those residues, Asp435, is equally important to the binding of ANG. Substitution of any two of these residues has a superadditive effect on ANG binding, but a subadditive effect on RNase A binding (Chen and Shapiro 1999).

Alterations to a second cluster of RI residues, including Trp261, Trp263, Trp318, and Trp375, have also been shown to display superadditive effects on ANG binding (Shapiro *et al.* 2000). Recent studies have reported superadditive effects in the RI·EDN complex (Teufel *et al.* 2003); both the C-terminal residues and tryptophan clusters contribute significantly to binding and demonstrate negative cooperativity, as in ANG binding. To date, no such negative cooperativity has been demonstrated for binding to RNase A (Chen and Shapiro 1999; Shapiro *et al.* 2000). These results suggest that the binding energy could be more widely distributed in the RI·RNase A complex than in the RI·EDN and RI·ANG complexes.

Structural and biochemical studies have provided significant evidence that the molecular interactions in RI·ribonuclease complexes differ substantially. For example, residues 408–410 in human RI appear to contact RNase A but not ANG. Remodeling these

residues to yield C408W/V409/G410W RI decreases the K_i value for RNase A and RNase 1 by >10^8-fold, but increases that value for ANG by only twofold (Kumar *et al.* 2004). Thus, the ligand specificity of RI can be altered dramatically by changing only a few residues. It is noteworthy that the C408W/V409/G410W variant of RI could be a useful tool for future studies on the biological function of ANG and the RI·ANG complex.

Cysteine Content and Oxidative Instability

LRR proteins commonly have N- and C-terminal domains that are rich in cysteine residues (Kobe and Kajava 2001). Still, only proteins from the RI-like and cysteine-containing LRR subfamilies contain cysteine residues in their consensus sequence (Kobe and Kajava 2001). Human RI and porcine RI contain 32 and 30 cysteine residues, respectively, comprising almost 7% of their amino acid residues (Hofsteenge *et al.* 1988; Lee *et al.* 1988). Sequence analysis of RI from human, pig, mouse and rat shows that 27 of the cysteine residues are conserved (Fig. 2). Several of the these cysteine residues could play key structural roles: the sulfhydryl group of the cysteine residue at position 10 of the A-type repeat appears to donate a hydrogen bond to the main-chain oxygen of residue 8, whereas the cysteine residue at position 17 of the A-type repeat is part of the hydrophobic core (Kobe and Deisenhofer 1994) (Fig. 3).

All of its cysteine residues must remain reduced for RI to maintain activity (Fominaya and Hofsteenge 1992). Oxidation of RI is a highly cooperative process (Fominaya and Hofsteenge 1992). Reaction of RI with a substoichiometric amount of 5,5-dithiobis(2-nitrobenzoic acid) (DTNB) yields a mixture of completely oxidized, inactive molecules and completely reduced, active molecules. Subsequent to oxidation of only a few cysteines, RI

rapidly undergoes a conformational change that results in increasing reactivity of the remaining thiols (Fominaya and Hofsteenge 1992). Several proximal cysteine residues create triggers for the oxidation and denaturation of RI. Replacing Cys328 and Cys329 with alanine residues endows RI with 10- to 15-fold greater resistance to oxidation by hydrogen peroxide with only a minimal effect on its affinity for RNase A (Kim *et al.* 1999).

Unlike unbound RI, the RI·RNase A complex can undergo partial oxidation (Ferreras *et al.* 1995). Treatment of the RI·RNase A complex with DTNB oxidizes up to 14 of its 30 cysteine residues and allows the enzyme to express up to 15% of its enzymatic activity. Only after dissociation does RI undergo its typical all-or-none oxidation. Thus, ribonucleases afford RI with some degree of protection from oxidation.

Degradation of RI correlates to its oxidative inactivation. Inducing oxidative damage in LLK-PC1 cells with hydrogen peroxide and diamide results in the degradation of RI (Blázuez *et al.* 1996). Similarly, oxidative stress in human erythrocytes induces decreased levels of glutathione followed by gradual loss of RI activity in the cytosol (Moenner *et al.* 1998). In contrast to LLK-PC1 cells, inactivated RI is detected in nascent Heinz bodies of human erythrocytes. Oxidation could be a mechanism by which the activity of RI (and thereby its cognate ribonucleases) is regulated in the cytosol.

Biological Activities

Expression Levels and Tissue Distribution. RI has been found in the cytosol of many cell types. Although it inhibits secretory ribonucleases, RI has not been detected in extracellular fluids, such as plasma, saliva, and urine (Nadano *et al.* 1994; Futami *et al.* 1997). The expression patterns of RI have been investigated extensively during the previous

three decades, with the hope of revealing insight into the biological role of RI. Still, the literature is full of conflicting conclusions. RI biosynthesis seems to correlate positively with anabolic activity, such as cell proliferation; increased RI levels have been found in rat liver after treatment with 2-acetamidofluorene to induce tumors (Wojnar and Roth 1965) and in developing neonatal rats (Suzuki and Takahashi 1970). Yet, RI levels are not elevated in SV-40–transformed hamster embryo fibroblast cells, stimulated HL-60 cells (Kyner *et al.* 1979), or many hepatocyte lines. The labile nature of RI could have compounded the difficulty of correlating RI levels with physiological relevance. A recent study did, however, find that high RI levels decreased angiogenesis and tumor formation in mouse xenographs (Botella-Estrada *et al.* 2001).

Role in Ribonuclease Cytotoxicity. In 1955, RNase A was found to be toxic to carcinomas in mice and rats (Ledoux 1955; Ledoux 1955). The antitumor activity of RNase A showed poor promise as a chemotherapeutic because milligram quantities were required to achieve a beneficial effect (Roth 1963). In 1973, the antitumor activity of dimeric BS-RNase towards Crocker tumor transplants in mice was discovered (Matousek 1973). Further characterization demonstrated, however, that BS-RNase is a poor candidate for cancer chemotherapy, as it has non-specific toxicity; is antispermatogenic (Matousek 1994), hinders embryo development (Matousek 1975) and oocyte maturation (Slavík *et al.* 2000), and is immunosuppressive (Matousek *et al.* 1995).

Amphibian ribonucleases from Rana pipiens (Darzynkiewicz *et al.* 1988), Rana catesbeiana (Nitta *et al.* 1987; Nitta *et al.* 1994), and Rana japonica (Nitta *et al.* 1994) were found to contain antitumor activity. Onconase® (ONC) is an RNase A homolog from Rana

pipiens and is both cytotoxic and cytostatic towards cultured tumor cells (Darzynkiewicz *et al.* 1988; Ardelt *et al.* 1991). ONC also causes the regression of xenographs in mice (Mikulski *et al.* 1990). ONC has been successful in the treatment of malignant mesothelioma in Phase I (Mikulski *et al.* 1993; Mikulski *et al.* 1995) and Phase II clinical trials (Mikulski *et al.* 2002). Side effects of ONC are reversible and include renal toxicity and proteinuria. Phase III clinical studies of ONC for the treatment of malignant mesothelioma are in progress.

ONC shares 30% amino acid sequence identity with RNase A (Ardelt *et al.* 1991). Although the key active-site residues of RNase A—His12, Lys41, His119—are conserved in ONC, the amphibian enzyme has ~0.1% of the ribonucleolytic activity of RNase A (Boix *et al.*, 1996; Bretscher *et al.*, 2000; Leland *et al.*, 2000). The ribonucleolytic activity of ONC is, however, essential for its cytotoxicity (Wu *et al.* 1993; Boix *et al.* 1996; Newton *et al.* 1997; Newton *et al.* 1998). The structure of crystalline ONC has been determined, and although ONC is twenty residues shorter than RNase A, the two enzymes share similar secondary and tertiary structure (Wlodawer 1985; Mosimann *et al.* 1994). Deletions within ONC are positioned within surface loops and at the N-terminus. ONC contains four disulfide bonds, three of which are present in RNase A. The synapomorphic disulfide bond in ONC secures its C-terminus, and is responsible for endowing ONC with remarkable conformational stability (Leland *et al.*, 2000; Notomista *et al.*, 2001). For example, the T_m value of ONC is 90 °C, which is 30 °C higher than that of RNase A.

The mechanism by which a ribonuclease is cytotoxic can be dissected into four steps: (1) cell-surface binding, (2) ribonuclease internalization, (3) translocation into the cytosol, and (4) evasion of RI and degradation of cellular RNA. ONC has low catalytic activity, but is a potent cytotoxin, suggesting that it accomplishes these four steps. In contrast, RNase A is

not an efficient toxin. Specifically, RNase A is $>10^3$-fold less cytotoxic to cells than is ONC (Wu *et al.* 1993). Both RNase A and ONC demonstrate nonspecific binding to the cell surface (K. A. Dickson and R. T. Raines, unpublished results) and no direct measurements of ribonuclease internalization and translocation to the cytosol have been reported to date. The distinguishing attribute of an RNase A homolog with cytotoxic activity is its ability to retain ribonucleolytic activity in the presence of RI. For example, RI does not associate with ONC but binds RNase A with nearly femtomolar affinity (Wu *et al.* 1993; Boix *et al.* 1996). As a result, ONC but not RNase A is capable of degrading cellular RNA and causing cell death.

The discovery of ONC in 1988 and its clinical success in subsequent years has intensified the study of other ribonucleases with biological actions. Current studies are focusing on understanding the mechanism of ribonuclease-mediated cytotoxicity with hope to improve potency and specificity. Using the cytotoxicity of ONC as a model, mammalian pancreatic ribonuclease variants have been endowed with toxic activity (for reviews, see (Youle and D'Alessio 1997; Leland and Raines 2001; Makarov and Ilinskaya 2003). The substantial difference in the binding affinities of ONC and RNase A for RI has proven to be a critical factor in the cytotoxicity of ribonucleases. Variants of pancreatic-type ribonucleases that have been engineered to evade RI possess cytotoxic activity. RI evasion has been achieved by covalently linking other proteins, dimerization, and site-directed mutagenesis.

The most common approach used to generate cytotoxic ribonucleases is to engineer amino acid substitutions that will disrupt contacts in the RI·ribonuclease complex specifically. For example, G88R RNase A is toxic to human leukemia cells (Leland *et al.* 1998). Invoking a similar strategy, RNase 1 has been engineered to contain a G88R-like surface loop (Leland *et al.* 1998). This variant evades RI and is also toxic to human leukemia

cells. Enhanced RI evasion can be attained at the expense of lower ribonucleolytic activity, as in K41R/G88R RNase A and A4C/K41R/G88R/V118C RNase A, without compromising cytotoxicity (Table II) (Bretscher *et al.* 2000; Dickson *et al.* 2003).

The ability of a ribonuclease to manifest its catalytic activity in the cytosol is related to its values of k_{cat}/K_M and K_d, and the concentration of RI in the cytosol ($[RI]_{cyto} = 4\ \mu M$ (Haigis *et al.* 2002). This ability can be described by the parameter $(k_{cat}/K_M)_{cyto}$, which is defined in Eq. (2) (Bretscher *et al.*, 2000; Raines, 1999; Futami *et al.*, 2002):

$$(k_{cat}/K_M)_{cyto} = (k_{cat}/K_M) / [1 + ([RI]_{cyto} / K_d)] \qquad (2)$$

The resulting values of $(k_{cat}/K_M)_{cyto}$ for RNase A, its variants, and ONC are listed in Table II. The most toxic RNase A variant reported to date has a double substitution in which Lys7 and Gly88 are replaced with alanine and arginine residues, respectively (Haigis *et al.* 2002). This variant demonstrates high catalytic activity, evades RI, and is nearly as toxic as ONC to human leukemia cells.

The role of RI in ribonuclease cytotoxicity has been examined directly by modulating intracellular levels of RI. Overexpression of RI in K-562 or HeLa cells diminished the potency of cytotoxic variants of RI without affecting the toxicity of ONC (Haigis *et al.* 2002). These findings suggest that ONC has no affinity for RI, such that $(k_{cat}/K_M)_{cyto} = k_{cat}/K_M$; upon entering a cell, ONC is able to degrade cellular RNA uninhibited. Conversely, the $(k_{cat}/K_M)_{cyto}$ values for RNase A variants that maintain affinity for RI are limited by the concentration of cytosolic RI.

Similar results were obtained using RNAi to suppress levels of cytosolic RI. Suppression resulted in increased susceptibility to ribonuclease variants that possess diminished affinity for RI (e.g., G88R RNase A), but did not endow ribonucleases with high

affinity for RI with cytotoxic activity (e.g., wild-type RNase A) (Monti and D'Alessio 2004). The amount of intact exogenous ribonuclease that reaches the cytosol of a cell is unknown, but likely to be small. Thus, even trace amounts of cytosolic RI could be sufficient to neutralize an invading ribonuclease with high affinity for RI.

Role in Angiogenesis. ANG is a unique ribonuclease (for reviews, see (Strydom 1998; Pavlov and Badet 2001; Riordan 2001). ANG acts on endothelial and smooth muscle cells to induce a wide range of cellular responses including cell proliferation, activation of cell-associated proteases, and cell migration and invasion. ANG binds to a receptor protein and is transported rapidly to the nucleus, where it activates transcription (Moroianu and Riordan 1994; Moroianu and Riordan 1994; Hu *et al.* 1997; Xu *et al.* 2002; Xu *et al.* 2003).

The role of RI in angiogenesis is controversial. The ribonucleolytic activity of ANG is weak (10^6-fold less than that of RNase A (Harper and Vallee 1989; Leland *et al.* 2002) but essential for its biological activity (Shapiro *et al.* 1989; Shapiro and Riordan 1989); amino acid substitutions that abolish ribonucleolytic activity also prevent angiogenesis. RI added extracellularly also inhibits angiogenesis (Shapiro and Vallee 1987; Polakowski *et al.* 1993), most likely by preventing ANG from binding to its receptor. Because the K_d value of the RI·ANG complex is among the lowest of known biomolecular interactions, RI could serve to protect cellular RNA from ANG that leaks inadvertently into the cytosol. On the other hand, RI could serve to control the biological activity of ANG. In one possible scenario, RI negatively regulates ANG that gains access to the cytosol; inactivation of RI reactivates ANG that was sequestered in an RI·ANG complex. Finally, the extraordinary affinity of ANG for RI suggests that the RI·ANG complex itself could have biological activity, though this hypothesis is contradicted by the known angiogenic activity of ANG in chick embryos, which

do not possess an RI that binds to mammalian ribonucleases (Kraft and Shortman 1970; Dijkstra *et al.* 1978).

Alternative Biological Roles. The marked oxidation sensitivity of RI in addition to its all-or-none mechanism of oxidative inactivation and denaturation is well documented (Fominaya and Hofsteenge 1992; Kim *et al.* 1999). Yet, the biological significance of these properties remains unclear. One hypothesis suggests that RI is an oxidation sensor in the cell. Overexpression of RI in rat glial cells conferred protection against hydrogen peroxideinduced stress, as indicated by the increased viability of cells, decreased leakage of lactate dehydrogenase, and increased content of reduced glutathione (Cui *et al.* 2003). Injection of RI into mice also conferred protection from per-oxidative injuries of the liver induced by exposure to carbon tetrachloride (Cui *et al.* 2003). These experiments suggest that RI could protect cells against two distinct onslaughts: invading ribonucleases and oxidative damage.

Surprisingly, significant quantities of RI have been detected in human erythrocytes, which are essentially devoid of ribonucleases and RNA (Moenner *et al.* 1998). The presence of RI in erythrocytes provides additional evidence that RI serves multiple roles in mammalian cells. Oxidative stress on isolated red blood cells resulted in reduced levels of glutathione followed by gradual loss of RI activity associated with its aggregation in Heinz bodies (Moenner *et al.* 1998). A similar sequence of inactivation and degradation has been noted for hemoglobin in response to oxidative stress (Allen and Jandl 1961) and other proteins (Strydom 1998) associated with aging. Decreases in RI activity have been observed in association with numerous diseases, including cataract formation (Cavalli *et al.* 1979), leukemia (Kraft and Shortman 1970), and exposure to ionizing radiation (Kraft *et al.* 1969).

Thus, RI in human erythrocytes, as well as nucleated cells, could be a determinant of cellular lifespan or simply a marker of aging.

Conclusions

RI possesses remarkable affinity for pancreatic-type ribonucleases, despite their limited sequence identity. The resulting noncovalent complexes are some of the tightest known in biology. Details of the molecular interactions within RI·ribonuclease complexes have been elucidated from structural and biochemical investigations. Moreover, RI is known to be a sentry, protecting mammalian cells against invading ribonucleases, which abound in extracellular fluids. Still, many questions remain regarding the biological activity of RI: Why have its Ki values evolved to be so low? What is the significance of the oxidation sensitivity of RI? Does the RI·ribonuclease complex itself have a biological role? In addition, the potential of the unique tertiary structure of RI to serve as a scaffold for the design of new receptors is virtually unexplored, but seemingly limitless. Accordingly, future research will likely be directed at elucidating the biological significance of the remarkable biochemical properties of RI, and developing RI as a scaffold for protein engineering. We look forward to learning the results of this effort.

Table 1. Kinetic parameters for RI inhibition of ribonucleases.

RI	Ribonuclease	k_a (M^{-1} s^{-1})	k_d (s^{-1})	K_i or K_D (M)	Method	Ref.
Human	ANG	1.8×10^{8}	1.3×10^{-7}	7.1×10^{-16}	Physical	a, b
	ANG	2.0×10^{8}	1.1×10^{-7}	5.4×10^{-16}	Physical	c
Human	RNase A	3.4×10^{8}	1.5×10^{-5}	4.4×10^{-14}	Physical/Enzymatic	a, b
	RNase A	3.4×10^{8}	1.2×10^{-5}	3.5×10^{-14}		a, b
	RNase 2	1.9×10^{8}	1.8×10^{-7}	9.4×10^{-16}		a, b
Porcine	RNase A	1.7×10^{8}	9.8×10^{-6}	5.9×10^{-14}	Enzymatic	d
	RNase A	1.3×10^{8}	1.5×10^{-5}	1.13×10^{-13}		e
	RNase A	—	—	7.4×10^{-14}		d
	RNase 4	1.5×10^{8}	1.3×10^{-7}	4.0×10^{-15}		f

a) From ref (Lee *et al.*, 1989a).
b) From ref (Lee *et al.*, 1989b).
c) From ref (Papageorgiou *et al.*, 1997).
d) From ref (Vicentini *et al*, 1990.)
e) From ref (Zelenko *et al.*, 1994).
f) From ref (Hofsteenge *et al.*, 1998).

Table 2. Properties of ribonuclease A, its variants, and Onconase®

Ribonuclease	k_{cat}/K_M (10^6 $M^{-1}s^{-1}$)	K_d (nM)	$(k_{cat}/K_M)_{cyto}$ (10^3 $M^{-1}s^{-1}$)	IC_{50} (μM)	Ref
Wild-type RNase A	43 ± 3	6.7×10^{-5}	0.00072	>50	a – c
G88R RNase A	14 ± 2	0.57 ± 0.05	2.0	10 ± 1	a – c
A4C/G88R/V118C RNase A	2.6 ± 0.2	1.3 ± 0.3	0.84	4.1 ± 0.6	c
K41R/G88R RNase A	0.6 ± 0.06	7.5 ± 1.8	1.1	5.2 ± 0.7	a – c
A4C/K41R/G88R/V118C RNase A	0.13 ± 0.03	27 ± 3.7	0.87	7.6 ± 0.9	c
K7A/G88R RNase A	8.8 ± 2.6	7.2 ± 0.4	15.8	1.0 ± 0.1	b
ONC	0.00035 ± 0.00010	≥1×10^6	>0.35	0.49 ± 0.06	b

a) From ref (Abel *et al.*, 2001)
b) From ref (Haigis *et al.*, 2002)
c) From ref (Dickson *et al.*, 2003)

Table 3. Characteristics of LRR protein subfamilies

Subfamily	Organism origin	Cellular location (Subfamily)	Representative Protein (organism)	Function	Length of typical LRR (range)	2° Structure of Interstrand Region	PDB code	Ref.
Typical	Animals, fungi	Extracellular	TSHR (human)	Receptor for thyrotropin	24 (20–27)	α-helix (model)	N.A	N.A.
RI-like	Animals	Intracellular	RI (pig)	Inhibits ribonucleases	28-29 (28–29)	α-helix	1BNH	a
Cysteine-Containing	Animals, plants, fungi	Intracellular	Skp2 (human)	Substrate binding in ubiquitination	26 (25–27)	α-helix	1FQV	b
Plant-Specific	Plants, primarily eukaryotes	Extracellular	Pgip (kidney bean)	Pathogen defense	24 (23–25)	3_{10} helix	1OGQ	c
SD22-like	Animals, fungi	Intracellular	U2A´ (human)	Splicing	22 (21–23)	3_{10} helix, α-helix	1A9N	d
Bacterial	Gram-negative bacteria	Extracellular	YopM (*Y. pestis*)	Virulence factor	20 (20–22)	Polyproline II	1G9U	e

a) From ref (Kobe and Deisenhofer, 1993).
b) From ref (Schulman *et al.*, 2000).
c) From ref (Matteo *et al.*, 2003).
d) From ref (Price *et al.*, 1998).
e) From ref (Evdokimov *et al.*, 2001).
f) From ref (Schott *et al.*, 2004).

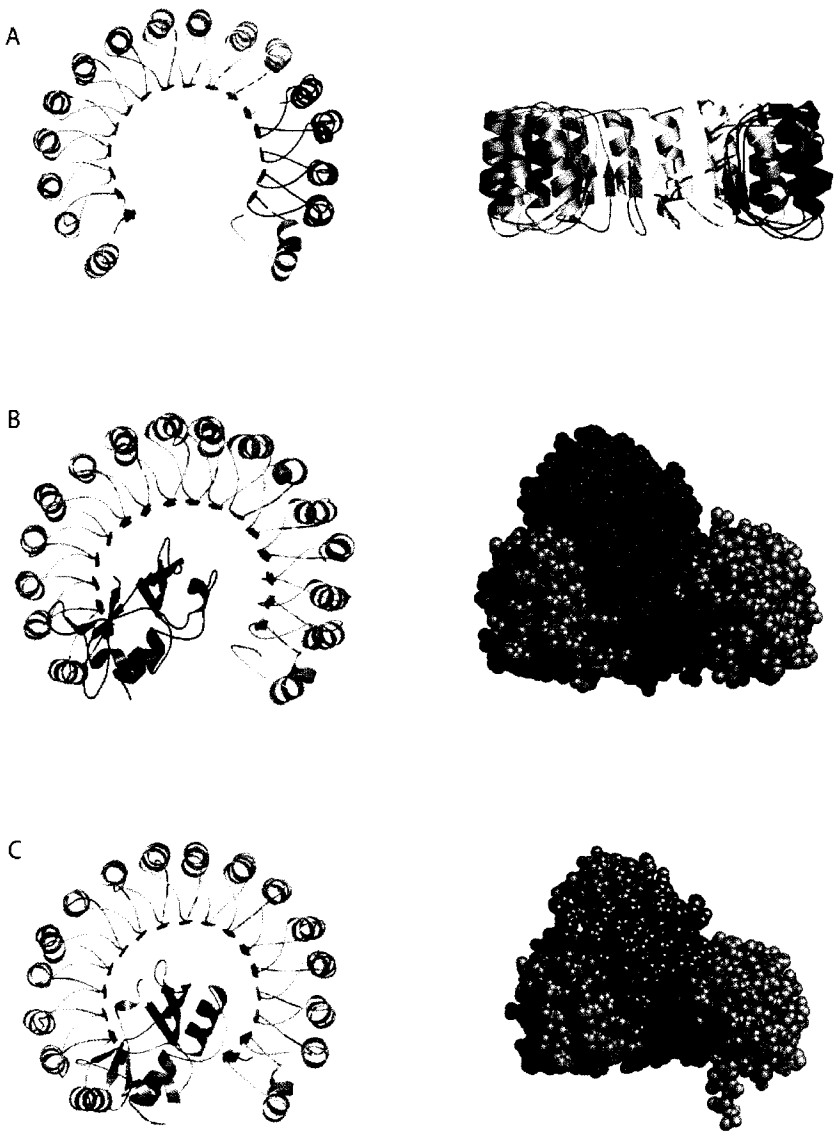

Figure 1.1 Three-dimensional structures of RI and its complexes with ribonucleases. (A) Porcine RI with colors corresponding to exon-encoded modules. (B) Porcine RI·RNase A complex. (C) Human RI·ANG complex.

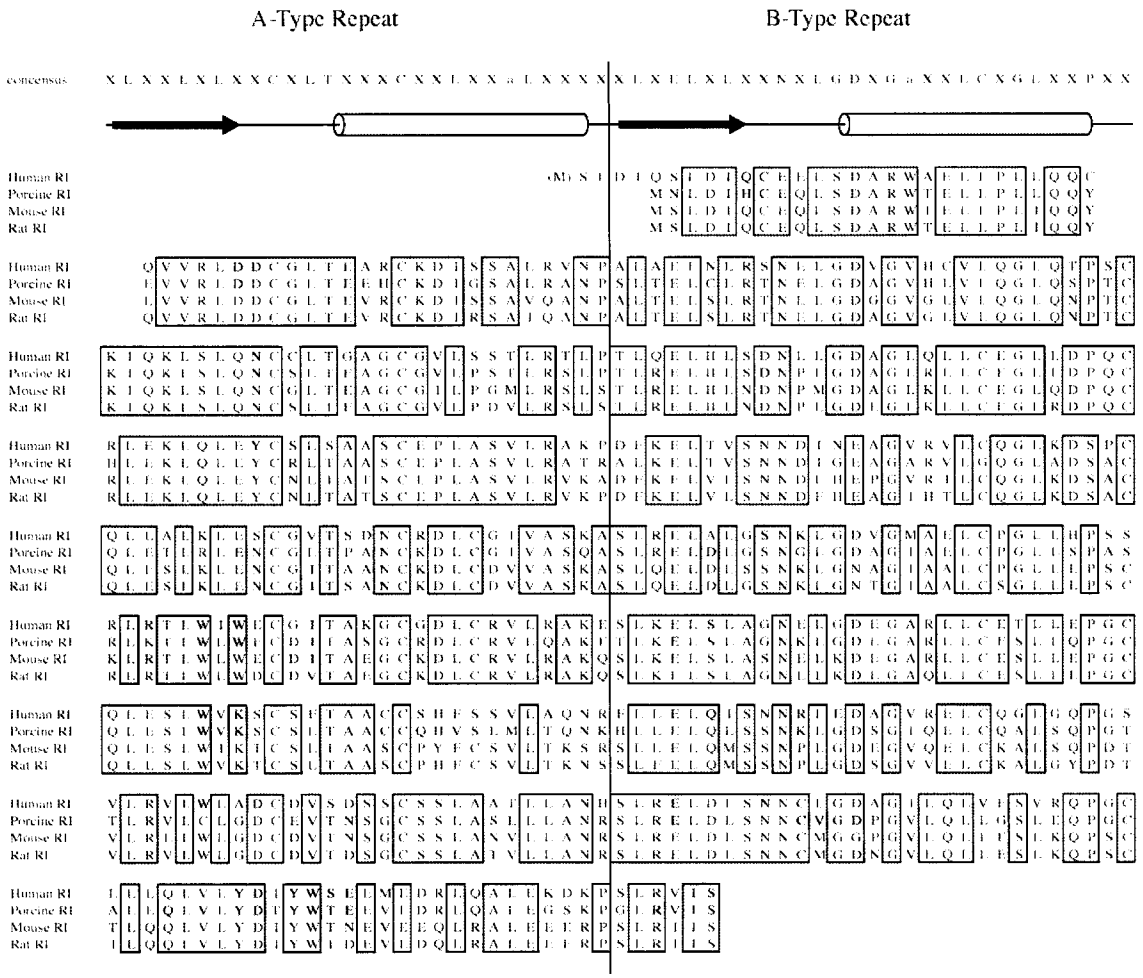

Figure 1.2 Alignment of the amino acid sequence of RI from human, porcine, mouse, and rat. The consensus sequence for the A-type and B-type repeats is indicated, along with the corresponding secondary structure. The initiator methionine residue was not detected in the N-terminal tryptic fragment of human RI and is shown in parentheses. Conserved residues are in boxes. Residues of human RI that contact ANG and residues of porcine RI that contact RNase A are shaded.

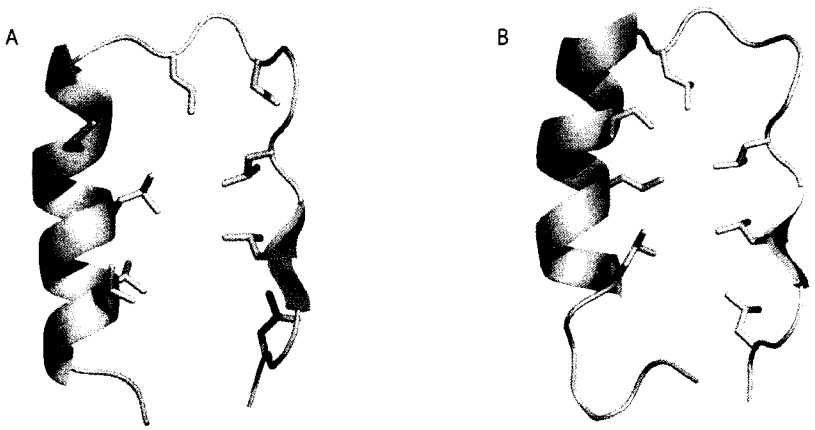

Figure 1.3. (A) A typical A-type repeat of RI (residues 138-165). (B) Typical B-type repeat (residues 223-252). The side chains of conserved aliphatic amino acids are shown.

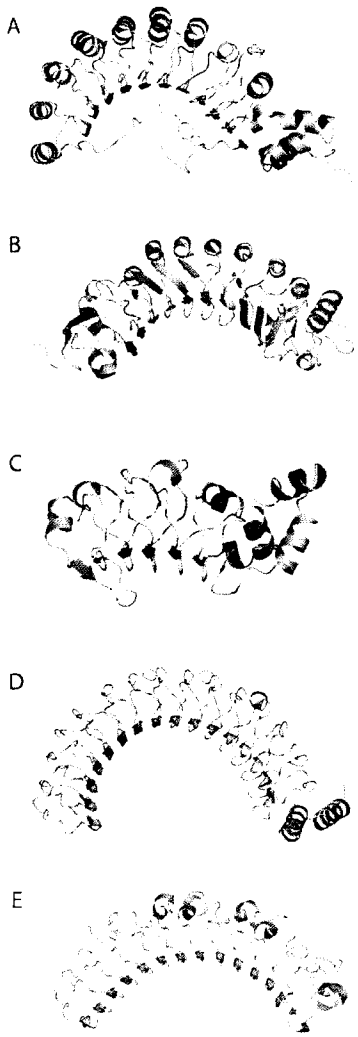

Figure 1.4 Structures of five representative LRR proteins (Table III). (A) Cysteine-containing protein Skp2. (B) Plant-specific protein Pgip. (C) SDS22-Like protein U2A′. (D) Bacterial protein YopM. (E) Decorin.

Chapter Two

Compensating effects on the cytotoxicity of ribonuclease A variants

Portions of this chapter were published as

Dickson, K. A., Dahlberg, C. L., and Raines, R. T. (2003) Compensating effects on the cytotoxicity of ribonuclease A variants. *Arch. Biochem. Biophys.* **415**, 172-177.

2.1 Abstract

Ribonuclease (RNase) A can be endowed with cytotoxic activity by enabling it to evade the cytosolic ribonuclease inhibitor protein (RI). Enhancing its conformational stability can increase further its cytotoxicity. The A4C/K41R/G88R/V118C variant of RNase A integrates four individual changes that decrease RI affinity (K41R/G88R) and increase conformational stability (A4C/V118C). Yet, the variant suffers a decrease in ribonucleolytic activity and is only as potent a cytotoxin as its precursors. Overall, cytotoxicity correlates well with the maintenance of ribonucleolytic activity in the presence of RI.

2.2 Introduction

Onconase® (ONC (Youle and D'Alessio 1997) is a homologue of bovine pancreatic ribonuclease (RNase A (Raines 1998). Isolated from the Northern leopard frog (*Rana pipiens*), ONC is now in Phase III clinical trials (USA) for the treatment of malignant mesothelioma (Mikulski *et al.* 2002). Although ONC is a potent antitumor agent, it has demonstrated dose-dependent renal toxicity (Mikulski *et al.* 1993; Mikulski *et al.* 1995). RNase A does not possess antitumor activity, but certain variants of RNase A (Leland *et al.* 1998; Bretscher *et al.* 2000; Klink and Raines 2000) and its human homologue (Leland *et al.* 2001) are toxic to tumor cells *in vitro*. Unlike ONC, mammalian ribonucleases are not retained in the kidney (Vasandani *et al.* 1996), and can therefore serve as the basis for new cancer chemotherapeutics (Leland and Raines 2001).

RNase A and ONC possess 30% amino acid identity (Ardelt *et al.* 1991) and have similar tertiary structures (Mosimann *et al.* 1994; Youle and D'Alessio 1997). Both RNase A and ONC catalyze the cleavage of the P–$O^{5¢}$ bond of RNA on the 3¢ side of pyrimidine nucleotides (Messmore *et al.* 1995). Two biochemical properties of ONC that are known to contribute to its cytotoxic activity are its conformational stability and its evasion of the cytosolic ribonuclease inhibitor protein (RI).

Three of the four disulfide bonds in RNase A are conserved in ONC. ONC possesses a fourth, synapomorphic disulfide bond that tethers the C-terminus to a central β-strand. Removal of this disulfide bond compromises the conformational stability as well as the cytotoxic activity of ONC (Leland *et al.* 2000). Likewise, incorporating a fifth disulfide that tethers the N- and C-termini of RNase A (Fig. 1) increases its conformational stability and cytotoxicity (Klink and Raines 2000).

To date, the known property of secretory ribonucleases that correlates most closely with cytotoxicity is the ability to evade RI. ONC binds weakly to RI (estimated $K_d^{app} \geq 10^{-6}$ M (Boix *et al.* 1996), but RNase A binds strongly to the inhibitor ($K_d = 6.7 \times 10^{-14}$ M (Vicentini *et al.* 1990). The difference in RI affinity can be attributed to subtle differences in sequence and structure. For example, many of the RNase A residues that contact RI are replaced by dissimilar residues in ONC (Kobe and Deisenhofer 1996; Leland *et al.* 1998). RNase A variants have been created that, like ONC, evade RI. For example, Gly88 of RNase A forms a close contact with Trp257 and Trp259 of RI (Fig. 1). Incorporating the large, hydrophilic amino acid arginine at position 88 results in a 10^4-fold decrease in affinity for RI (Leland *et al.* 1998). Similarly, Lys41 of RNase A interacts with Tyr430 and Asp431 of RI (Fig. 1). Replacing Lys41 with arginine results in an additional 20-fold decrease in RI affinity (Bretscher *et al.* 2000).

Catalytic activity must be maintained to retain cytotoxicity. Lys41 of RNase A plays an important role in catalysis by donating a hydrogen bond to a non-bridging phosphoryl oxygen in the transition state during RNA cleavage (Messmore *et al.* 1995). The K41R substitution disrupts the RI•RNase A complex, but also reduces k_{cat}/K_M by 30-fold relative to G88R RNase A (Bretscher *et al.* 2000). Still, the 20-fold increase in its K_d value for binding to RI is sufficient to produce a more potent ribonuclease. These data imply that cytotoxicity can be retained in an RNase A variant with decreased catalytic activity if there is a concomitant decrease in affinity for RI.

Here, we attempt to maximize the cytotoxic potency of RNase A by enhancing *both* its ability to evade RI and its conformational stability. Specifically, we combine the K41R and G88R substitutions intended to disrupt the RI•RNase A complex with a fifth disulfide bond

that tethers the N- and C-termini. The results reveal that an interplay exists βween these two biochemical properties and provide guidance for the development of new cytotoxic ribonucleases.

2.3 Materials and methods

Materials. E. coli strain BL21(DE3) and the pET22b(+) expression vector were from Novagen (Madison, WI). *E. coli* strain TOPP 3 (Rif^r [F′ *proAB lacI*^{q}ZΔ*M15* Tn10 (Tet^r) (Kan^r)]), which is a non–K-12 strain, was from Stratagene (La Jolla, CA). Enzymes for DNA manipulations were from Promega (Madison, WI) or New England BioLabs (Beverly, MA). Oligonucleotides and 6-FAM~(dA)rU(dA)$_2$~6-TAMRA, where 6-FAM refers to 6-carboxyfluorescein and 6-TAMRA refers to 6-carboxytetramethylrhodamine, were from Integrated DNA Technologies (Coralville, IA). K-562 cells, which were derived from a human chronic myelogenous leukemia, were from the American Type Culture Collection (Manassas, VA). [*methyl*-^{3}H]Thymidine (6.7 Ci/mmol) was from NEN Life Sciences (Boston, MA). All other chemicals and biochemicals were of commercial grade or βter, and were used without further purification.

Instruments. Absorbance measurements were made with a Cary 3 double-beam spectrophotometer equipped with a Cary temperature controller (Varian, Palo Alto, CA). Fluorescence measurements were carried out on a QuantaMaster 1 photon-counting fluorometer equipped with sample stirring (Photon Technology International, South Brunswick, NJ). Radioactivity was measured with a Beckman model LS 3801 liquid scintillation counter from Beckman Instruments (Fullerton, CA).

Preparation of proteins. Plasmids that direct the production in *E. coli* of wild-type RNase A (delCardayré *et al.* 1995), its G88R (Leland *et al.* 1998), A4C/G88R/V118C (Klink and Raines 2000), and K41R/G88R variants (Bretscher *et al.* 2000), and ONC (Leland *et al.* 1998) were described previously. Site-directed mutagenesis of the plasmid encoding A4C/G88R/V118C RNase A with oligonucleotide GTGCACAAAGGTGTTAACTGG**ACG**GCATCTATCTTTGGT was used to replace the AAG codon of Lys41 with a codon for arginine (reverse complement in boldface).

Proteins were prepared as described previously (delCardayré *et al.* 1995; Leland *et al.* 1998; Bretscher *et al.* 2000; Klink and Raines 2000), except that RNase A variants possessing the G88R substitution were refolded in the presence of 0.5 M arginine instead of 0.1 M NaCl. Ribonucleases were dialyzed extensively against phosphate-buffered saline (PBS) for use in all cytotoxicity and RI-binding assays.

Ribonuclease concentrations were determined by UV spectroscopy using $\varepsilon = 0.72$ ml·mg^{-1}cm^{-1} at 277.5 nm for RNase A (Sela *et al.*, 1957) and its variants and $\varepsilon = 0.87$ ml·mg^{-1}cm^{-1} at 280 nm for ONC (Leland *et al.* 1998).

Porcine RI was produced as described previously (Klink *et al.* 2001). The concentration of active RI was determined by its titration with RNase A.

Assays of conformational stability. The reversible thermal denaturation of A4C/K41R/G88R/V118C RNase A was monitored by using UV spectroscopy (Eberhardt *et al.* 1996). Specifically, the A_{287} of a 0.4 mg/mL solution of ribonuclease was monitored as the temperature of the solution was increased from 25 to 80°C in 1-°C increments. The data were fitted to a two-state model for denaturation using the program THERMAL (Varian, Palo Alto, CA). The value of T_m is the temperature at the midpoint of the thermal transition βween the native and unfolded states.

Assays of ribonucleolytic activity. The catalytic activity of ribonucleases was measured with the fluorogenic substrate 6-FAM~dArUdAdA~6-TAMRA (Kelemen *et al.*,999). Cleavage of this substrate results in a ~200-fold increase in fluorescence intensity (excitation at 492 nm; emission at 515 nm). Assays were performed at 23°C in 2.0 mL of 0.10 M MES–NaOH buffer (pH 6.0) containing NaCl (0.10 M), 6-FAM~dArUdAdA~6-TAMRA (50 nM), and enzyme (5–500 pM). Data were fitted to the equation: $k_{cat}/K_M = (\Delta I/\Delta t)/\{(I_f - I_0)[E]\}$ where $\Delta I/\Delta t$ is the initial velocity of the reaction, I_0 is the fluorescence intensity prior to the addition of enzyme, I_f is the fluorescence intensity after complete hydrolysis with excess wild-type enzyme, and [E] is the ribonuclease concentration.

Assays of ribonuclease inhibitor binding. The fluorescence of fluorescein-labeled A19C/G88R RNase A (fluorescein~G88R RNase A) decreases by nearly 20% upon binding to RI (Abel *et al.* 2001). A competition assay exploiting this property was used to determine the affinity of a each (unlabeled) RNase A variant for RI. Briefly, fluorescein~G88R RNase A (50 nM (Abel *et al.* 2001) and an RNase A variant (1 nM–2 μM) were incubated in 2.0 mL of PBS for 30 min at 23°C. The fluorescence intensity (excitation at 491 nm; emission at 511 nm) was measured before and after the addition of RI (to 50 nM). Values of

K_d for the complex βween RNase A variants and RI were determined as described previously (Abel *et al.* 2001).

Assays of cytotoxicity. The cytotoxicity of ribonucleases was determined by monitoring the incorporation of [*methyl*-^{3}H]thymidine into the newly synthesized DNA of K-562 cells (Leland *et al.* 1998). Briefly, cells were maintained at 37°C in RPMI media containing FBS (10% v/v), penicillin (100 units/ml), and streptomycin (100 μg/ml). Ribonucleases were incubated with K-562 cells for 44 h at 37°C. [*methyl*-^{3}H]Thymidine (0.4 μCi/well) was added for 4 h, after which cells were harvested onto a glass fiber filter and counted. [*methyl*-^{3}H]Thymidine incorporation in cells incubated in the absence of ribonuclease was used to define 100% ^{3}H incorporation. IC_{50} values were calculated by fitting the data to the equation: $S = 100 \times IC_{50}/(IC_{50} + [\text{ribonuclease}])$, where S is the percent of [*methyl*-^{3}H]thymidine incorporated after a 48-h incubation with a ribonuclease (Haigis *et al.* 2002).

2.4 Results

Conformational stability. Values of T_m for RNase A, its variants, and ONC are listed in Table 1. The T_m of A4C/K41R/G88R/V118C RNase A was 67.0°C. Thus, the increase in T_m achieved by installing a fifth disulfide bond in G88R RNase A and K41R/G88R RNase A is similar.

Ribonucleolytic activity. Values of k_{cat}/K_M values for RNase A, its variants, and ONC are listed in Table 1. The k_{cat}/K_M of A4C/K41R/G88R/V118C RNase A was 1.3 ¥ 10^5 $M^{-1}s^{-1}$, which is 330-fold lower than that of wild-type RNase A. The k_{cat}/K_M values for wild-type RNase A, its other variants, and ONC are similar to those reported previously (Bretscher *et*

al. 2000; Klink and Raines 2000).

Ribonuclease inhibitor binding. Values of K_d for complexes of RI with RNase A and its variants are listed in Table 1. The complex of RI with A4C/K41R/G88R/V118C RNase A has $K_d = 27$ nM. This value is the highest yet reported for a variant of RNase A, and is nearly 10^6-fold greater than that for wild-type RNase A (Vicentini *et al.* 1990). The K_d values for wild-type RNase A, its other variants, and ONC are similar to those reported previously (Bretscher *et al.* 2000; Klink and Raines 2000).

The K_d values were used to calculate the change in the free energy of association ($\Delta\Delta G$) for RI with each of the RNase A variants. These $\Delta\Delta G$ values are listed in Table 1.

Cytotoxicity. Data on the cytotoxicity of RNase A, its variants, and ONC are shown in Fig. 2, and the resulting IC_{50} values are listed in Table 1. The IC_{50} values for all four toxic variants of RNase A vary by only 2.4-fold. Surprisingly, A4C/K41R/G88R/V118C RNase A was less cytotoxic ($IC_{50} = 7.6$ μM) than either K41R/G88R RNase A or A4C/G88R/V118C RNase A. The IC_{50} values for the other RNase A variants and ONC are in gratifying agreement with those reported previously (Bretscher *et al.* 2000; Klink and Raines 2000).

$(k_{cat}/K_M)_{cyto}$. The ability of a ribonuclease to manifest its catalytic activity in the cytosol is related to its values of k_{cat}/K_M and K_d. This ability can be described by the parameter $(k_{cat}/K_M)_{cyto}$ (Raines 1999; Bretscher *et al.* 2000; Futami *et al.* 2002; Haigis and Raines 2003):

$$(k_{cat}/K_M)_{cyto} = (k_{cat}/K_M)/[1+([RI]_{cyto}/K_d)] \quad (1)$$

The value of $[RI]_{cyto}$ was estimated to be 4 μM by assuming that RI constitutes 0.08% of cytosolic protein (Haigis *et al.* 2002) and that the total concentration of protein in the cytosol

is 250 mg/ml (Ellis 2001). The resulting values of $(k_{cat}/K_M)_{cyto}$ for RNase A, its variants, and ONC are listed in Table 1.

2.5 Discussion

Ribonucleases exert their cytotoxic activity in the cytosol of the cell. To be cytotoxic, a ribonuclease must maintain its ribonucleolytic activity (and hence its conformational stability) so as to degrade cellular RNA, even in the presence of RI. We have created an RNase A variant (A4C/K41R/G88R/V118C RNase A) that combines changes that confer conformational stability and the ability to evade cellular RI.

Many of the residues in RNase A that are most important for substrate binding and catalysis participate in intermolecular interactions with RI (Kobe and Deisenhofer 1996). Our data provide direct experimental support for this dichotomy. We find that values of k_{cat}/K_M for RNase A variants decrease in the order: G88R > A4C/G88R/V118C > K41R/G88R > A4C/K41R/G88R/V118C (Table 1). Values of K_d demonstrate exactly the opposite trend. Hence for these variants, ribonucleolytic activity is related inversely to the ability to evade RI. In other words, disrupting the RI•RNase A complex compromises catalytic activity.

The conformational stability afforded by the incorporation of the fifth disulfide bond in G88R RNase A leads to a more cytotoxic variant (Klink and Raines 2000). Yet, the addition of the same disulfide bond to K41R/G88R RNase A results in a less cytotoxic variant (Table 1). The fifth disulfide bond also decreases the value of k_{cat}/K_M by 5-fold. Apparently, the benefit of enhanced conformational stability cannot always overcome a decrease in k_{cat}/K_M to generate a more cytotoxic ribonuclease.

The value of $(k_{cat}/K_M)_{cyto}$ reports on the ribonucleolytic activity of a ribonuclease in the cytosol (Raines 1999; Bretscher *et al.* 2000; Futami *et al.* 2002; Haigis and Raines 2003). Values of $(k_{cat}/K_M)_{cyto}$ vary by <3-fold for the four cytotoxic RNase A variants (Table 1). Likewise, values of IC_{50} vary by <3-fold for these four variants. These small variations are in marked contrast to the nearly 10^3-fold variation in the values of both k_{cat}/K_M and K_d. Thus, $(k_{cat}/K_M)_{cyto}$ correlates much more closely with IC_{50} than does either k_{cat}/K_M or K_d. Only the parameter $(k_{cat}/K_M)_{cyto}$, which takes into account both (k_{cat}/K_M) and K_d, provides a reliable forecast for the cytotoxicity of an RNase A variant.

What is the limit to the cytotoxicity of an RNase A variant? Suppose a variant could maintain the k_{cat}/K_M value of wild-type RNase A and have $K_d >> 4\ \mu M$. Then according to Eq. 1 and the data in Table 1, its $(k_{cat}/K_M)_{cyto} = 4.3 \times 10^7\ M^{-1}s^{-1}$. This value is 5×10^4-fold greater than that of the A4C/G88R/V118C, K41R/G88R, or A4C/K41R/G88RV118C variant. If IC_{50} is truly inversely proportional to $(k_{cat}/K_M)_{cyto}$, then such an RNase A variant would have an $IC_{50} = 5\ \mu M/5 \times 10^4 = 0.1$ nM for K-562 cells. This IC_{50} value is much less than that of ONC (Table 1). Of course, this analysis is simplistic. Many other factors, including conformational stability (Klink and Raines 2000), are known to affect cytotoxicity. Still, this analysis provides both an inspiration for the design of new ribonuclease-based cytotoxins and a benchmark with which to gauge the success of those designs.

Overcoming inhibition by RI in the cytosol is an even more formidable task than is apparent from the K_d values listed in Table 1.The cytosol is crowded with macromolecules (Zimmerman and Minton 1991; Ellis 2001). The relatively low concentration of water there favors the formation of intermolecular complexes, thereby effectively lowering values of K_d. For example, the K_d value for the dimerization of a typical 40-kDa spherical protein is

reduced by 4- to 8-fold in the *E. coli* cytosol (Zimmerman and Minton 1991). Because far more surface area is buried in the RI·RNase A complex than in a typical protein–protein interaction (Kobe and Deisenhofer 1995), the RI·RNase A complex is likely to be significantly more stable in the cytosol than in the dilute solution of *in vitro* assays.

A4C/K41R/G88R/V118C RNase A has an enhanced ability to evade RI and greater conformational stability than its precursors. These attributes are offset by diminished catalytic activity. These compensating effects endow A4C/K41R/G88R/V118C RNase A with cytotoxic activity that differs by <3-fold from that of the G88R, A4C/G88R/V118C, and K41R/G88R variants, despite a nearly 10^3-fold variation in the values of both k_{cat}/K_M and K_d. Thus, increasing the cytotoxicity of RNase A (or its human homologue) requires diminishing its affinity for RI without compromising its conformational stability or catalytic activity.

Table 1

Properties of ribonuclease A, its variants, and Onconase®

Ribonuclease	T_m[a] (°C)	k_{cat}/K_M[b] (10^6 $M^{-1}s^{-1}$)	K_d[c] (nM)	$\Delta\Delta G$[c] (kcal/mol)	$(k_{cat}/K_M)_{cyto}$ (10^3 $M^{-1}s^{-1}$)	IC_{50}[d] (μM)
Wild-type RNase A	63.0[e]	43 ± 3[h]	6.7 ′ 10^{-5}[i]	0.0	0.00072	>50
G88R RNase A	64.0[e]	14 ± 2	0.57 ± 0.05[j]	5.3	2.0	10 ± 1
A4C/G88R/V118C RNase A	68.8[f]	2.6 ± 0.2	1.3 ± 0.3	5.8	0.84	4.1 ± 0.6
K41R/G88R RNase A	63.0[g]	0.6 ± 0.06	7.5 ± 1.8	6.8	1.1	5.2 ± 0.7
A4C/K41R/G88R/V118C RNase A	67.0	0.13 ± 0.03	27 ± 3.7	7.6	0.87	7.6 ± 0.9
ONC	90.0 [e]	0.00035 ± 0.00010[h]	≥1 ′ 10^6 [k]	>14	>0.35	0.49 ± 0.065

[a]Value of T_m were determined by UV (RNase A and its variants) or CD (ONC) spectroscopy.
[b]Values of k_{cat}/K_M (±S.E.M.) are for catalysis of 6-FAM~dArU(dA)$_2$~6-TAMRA cleavage at pH 6.0 and 23°C.
[c]Values of K_d (±S.E.M.) and $\Delta\Delta G = RT\ln(K_d/K_d^{\text{wild-type RNase A}})$ are for the complex with porcine RI at 23°C.
[d]Values of IC_{50} (±S.E.M.) are for cytotoxicity to human chronic myelogenous leukemia line K-562.
[e]Ref (Leland *et al.*, 1998). [f]Ref (Klink *et al.*, 2000). [g]Ref (Bretscher *et al.*, 2000. [h]Ref (Haigis *et al.*, 2002. [i]Ref (Vicentini *et al.*, 1990). [j]Ref (Abel *et al.*, 2002). [k]Ref (Boix *et al.*, 1996).

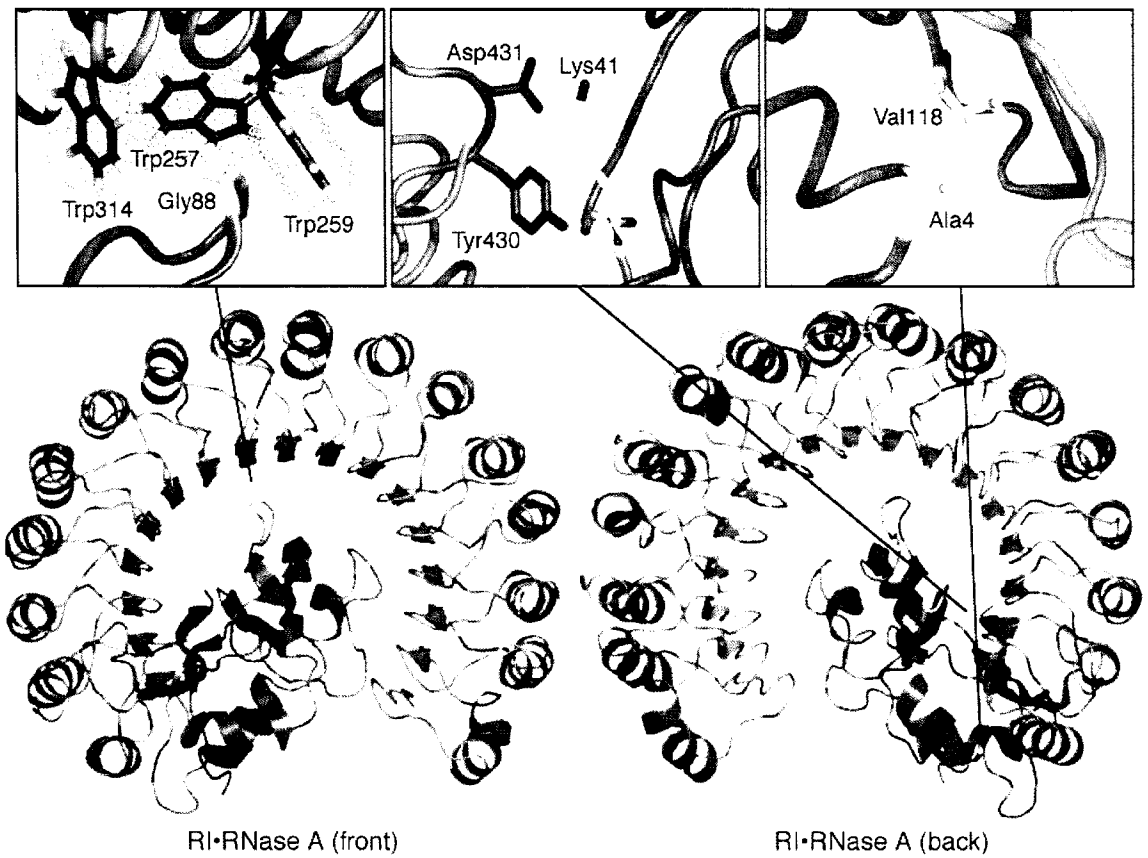

Figure 2.1 Interactions in the complex of RI (blue mainchain; purple sidechains) and RNase A (green mainchain; yellow sidechains). Images were created by using the atomic coordinates from Protein Data Bank entry 1DFJ (Kobe and Deisenhofer, 1995).

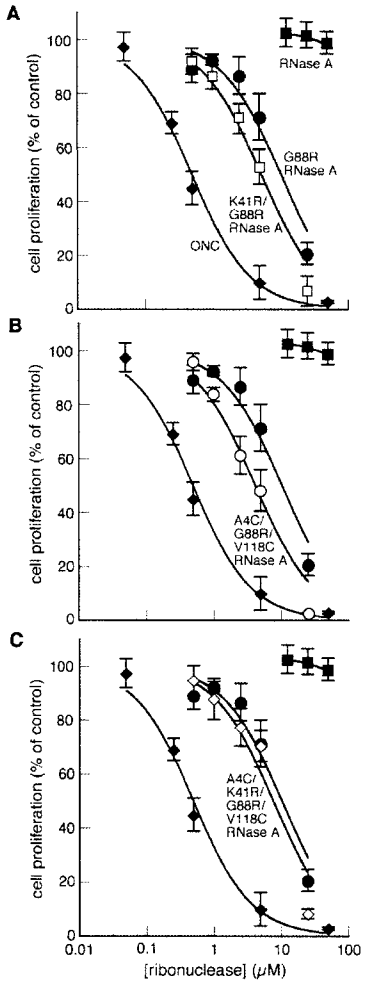

Figure 2.2 Effect of ribonucleases on the proliferation of K-562 cells. Cell proliferation was measured by [*methyl*-^{3}H]thymidine incorporation into cellular DNA after a 44-h incubation at 37°C with a ribonuclease. Values are the mean (± S.E.M.) of at least three independent experiments with triplicate samples and are expressed as a percentage of control cultures lacking an exogenous ribonuclease. For comparison, data for wild-type RNase A (closed squares), its G88R variant (closed circles), and Onconase® (closed diamonds) are depicted in each panel.

Chapter Three

Ribonuclease Inhibitor Regulates Neovascularization by Human Angiogenin

3.1 Abstract

Angiogenin (ANG) is a homolog of bovine pancreatic ribonuclease (RNase A) that induces neovascularization. Unique to the RNase A superfamily, ANG is the only ribonuclease with angiogenic activity and the only human angiogenic factor that possesses ribonucleolytic activity. To stimulate blood vessel growth, ANG must be transported to the nucleus and must retain its catalytic activity. Like other mammalian members of the RNase A superfamily, ANG forms an extremely tight complex ($K_d \approx 1$ fM) with the cytoplasmic ribonuclease inhibitor (RI). To explore whether RI affects ANG-induced angiogenesis, we created G85R/G86R ANG, which possesses 10^6-fold weaker affinity for RI yet retains wild-type levels of ribonucleolytic activity. G65R/G86R ANG was translocated to the nucleus of HUVE cells and stimulated cell migration of HUVE cells at lower protein concentrations than did wild-type ANG. Moreover, neovascularization of rabbit cornea by G85R/G86R ANG was more rapid and more pronounced than in eyes implanted with wild-type ANG. These results indicate that RI serves to regulate the biological activity of ANG.

3.2 Introduction

Angiogenin (ANG) is potent inducer of blood vessel growth (Fett *et al.* 1985) and has been implicated in the establishment, growth, and metastasis of tumors (Olson *et al.* 2001; Olson *et al.* 2002). A homolog of bovine pancreatic ribonuclease (RNase A (Raines 1998); EC 3.1.27.5), ANG is the only human angiogenic factor that possesses ribonucleolytic activity. ANG was first isolated from the conditioned medium of human adenocarcinoma cells (Fett *et al.* 1985) but is present in normal human plasma (Bläser *et al.* 1993) as well as numerous other tissues and organs (Moenner *et al.* 1994). In endothelial and smooth muscle cells, ANG induces a wide range of cellular responses including transcriptional activation (Xu *et al.* 2002), differentiation (Jimi *et al.* 1995), cell migration and invasion (G.-F. *et al.* 1994), and tube formation (Jimi *et al.* 1995). Upon binding to endothelial cells, a nuclear localization sequence (NLS), RRRGL, directs ANG to the nucleus where it accumulates rapidly (Moroianu and Riordan 1994). The nuclear localization and ribonucleolytic activity of ANG are both required for angiogenic activity (Moroianu and Riordan, 1994; Shapiro *et al*, 1989).

The ribonuclease inhibitor (RI), a cytosolic protein found in all mammalian tissues analyzed to date, binds to mammalian ribonucleases with extraordinary affinity (for reviews see (Roth 1967; Lee and Vallee 1993; Hofsteenge 1997; Shapiro 2001; Dickson *et al.* 2005). In particular, the RI·ANG complex (Papageorgiou *et al.* 1997) (Fig. 1) is the tightest known RI·ribonuclease complex ($K_d \approx 1$ fM) (Lee *et al.* 1989; Lee *et al.* 1989; Papageorgiou *et al.* 1997) and one of the tightest non-covalent interactions identified in biology. Binding of RI to ANG blocks the active site of the enzyme and completely abolishes its ribonucleolytic activity (Shapiro and Vallee 1987; Papageorgiou *et al.* 1997).

The role of RI in angiogenesis is controversial. RI added extracellularly inhibits angiogenesis (Shapiro and Vallee 1987). The ribonucleolytic activity of ANG is weak (10^6-fold less than that of RNase A) but essential for its biological activity; amino acid substitutions that eliminate ribonucleolytic activity also prevent angiogenesis (Shapiro *et al*, 1989; Leland *et al*, 2002; Shapiro *et al*, 1986). RI could serve to protect cellular RNA from ANG that leaks into the cytosol. Alternatively, RI could control ANG-induced neovascularization by regulating its catalytic activity.

The route by which ANG is transported from the cell surface to the nucleus is poorly understood. Homologs of ANG, including RNase A, human pancreatic ribonuclease (RNase 1), bovine seminal ribonuclease (BS-RNase), and Onconase (ONC), do not possess a NLS and, thus, are not routed to the nucleus. Instead, these ribonucleases are internalized by cells and gain access to the cytosol, where they encounter RI (Leland *et al*, 2001; Matousek *et al*, 2001; Rybak *et al*, 1999; Haigis *et al*, 2003). ONC, which does not bind to RI, can degrade cellular RNA and kill the cell (Darzynkiewicz *et al.* 1988). Likewise, variants of RNase A, RNase 1, and BS-RNase that have been engineered to evade RI demonstrate similar toxicity (for recent reviews, see (Leland and Raines 2001; Makarov and Ilinskaya 2003; Matou_ek *et al.* 2003). For example, Gly 88 of RNase A makes close contacts with three Trp residues of RI. Replacing Gly 88 with Arg disrupts the RI·RNase A complex and results in a 10^4-fold increase in K_d. The resulting G88R RNase A variant displays potent cytotoxic activity (Leland *et al.* 1998). Here, we explore the role of RI in ANG-induced angiogenesis by creating a variant of ANG that evades cytosolic RI.

3.3 Materials and Methods

Materials. Escherichia coli strain BL21(DE3) and the pET22b(+) expression vector were from Novagen (Madison, WI). E. coli strain TOPP 3 (Rif^r [F′ proAB lacI^{q}ZΔM15 Tn10 (Tet^r) (Kan^r)]), which is a non–K-12 strain, was from Stratagene (La Jolla, CA). Enzymes for DNA manipulations were from Promega (Madison, WI) or New England BioLabs (Beverly, MA). Oligonucleotides and 6-FAM~dArUdAdA~6-TAMRA, where 6-FAM refers to 6-carboxyfluorescein and 6-TAMRA refers to 6-carboxytetramethylrhodamine, were from Integrated DNA Technologies (Coralville, IA). Endothelial cell growth medium (EGM) and endothelial cell basal medium (EBM-2, Mg^{2+} and Ca^{2+} free) were purchased from Clonetics (San Diego, CA). All other chemicals and biochemicals were of commercial grade or βter, and were used without further purifications.

Instruments. Absorbance measurements were made with a Cary model 50 spectrophotometer (Varian, Sugarland, TX). Fluorescence was measured with a QuantaMaster1 photon-counting spectrophotometer from Photon Technology International (South Brunswick, NJ). Microscopy was performed with a LSM 510 confocal laser scanning microscopy (Carl Zeiss, Thornwood, NJ).

Preparation of proteins. Plasmids that direct the production in *E. coli* of wild-type RNase A, G88R RNase A, and ANG were described previously (Leland *et al.* 1998; Leland *et al.* 2002). Site-directed mutagenesis of the plasmid encoding ANG with the oligonucleotide AGGCCAGGGAGA**TCTTCT**ATGTAGCTT was used to substitute Gly 85 and 86 with Arg (reverse complement in boldface).

Ribonucleases and porcine RI were prepared as described previously (Leland *et al.* 1998; Klink *et al.* 2001; Leland *et al.* 2002), except that ANG was refolded in the

presence of 0.1 M NaCl instead of 0.5 M arginine. Ribonuclease concentrations were determined by UV spectroscopy using $\varepsilon = 0.72$ mg·ml^{-1}cm^{-1} at 277.5 nm for RNase A (Sela *et al.* 1957) and G88R RNase A and $\varepsilon = 0.83$ mg·ml^{-1}cm^{-1} at 280 nm for ANG and G85R/G86R ANG (Leland *et al.* 2002). Ribonucleases were dialyzed extensively against phosphate-buffered saline (PBS) prior to use in all RI-binding assays as well as all cell-based assays.

Enzymatic activity. For measurements of enzymatic activity, trace amounts of contaminating ribonucleases were separated from ANG and G85R/G86R ANG by chromatography on a dedicated HiTrap SP cation-exchange column equipped with an LKB peristaltic pump (Amersham-Pharmacia) as previously described (Leland *et al.* 2002). In addition to using DEPC-treated buffers, all tubing and glassware were treated with RNase Erase (MP Biomedicals, Aurora, OH) and rinsed extensively with DEPC-treated ddH_2O prior to column chromatography. The catalytic activity of ribonucleases was measured with the fluorogenic substrate 6-FAM~dArUdAdA~6-TAMRA (Kelemen *et al.* 1999). Cleavage of this substrate results in a ~200-fold increase in fluorescence intensity (excitation at 492 nm; emission at 515 nm). Assays were performed at 23°C in 0.1 M MES–NaOH buffer at pH 6.0, containing NaCl (0.10 M), 6-FAM~dArUdAdA~6-TAMRA, and enzyme. Data were fitted to the equation $k_{cat}/K_m = (\Delta I/\Delta t)/\{(I_f\text{-}I_0)[E]\}$, where $\Delta I/\Delta t$ is the initial velocity of the reaction, I_0 is the fluorescence intensity prior to the addition of enzyme, I_f is the fluorescence intensity after complete hydrolysis with excess RNase A, and [E] is the ribonuclease concentration.

Zymogram electrophoresis. Zymogram electrophoresis was performed as described previously to confirm that purified ANG and G85R/G86R were free from contaminating ribonucleolytic activity (Ribó *et al.* 1991; Leland *et al.* 2002). Briefly, ANG samples were

subjected to standard SDS–PAGE with the following modifications: the reducing agent was omitted from the sample buffer and the gel was copolymerized with poly(C) (0.5 mg/ml), which is a substrate for ANG and RNase A. After electrophoresis, SDS was removed from the gel by washing (2 x 10 min) with 10 mM Tris–HCl buffer at pH 7.5, containing 2-propanol (20% v/v). Ribonucleases were renatured by washing (2 x 10 min) with 10 mM Tris–HCl buffer pH 7.5, and then washing (15 min) with 0.1 M Tris–HCl buffer at pH 7.5. The gel was stained for 1 min with 10 mM Tris–HCl buffer pH 7.5, containing 0.2% toluidine blue, which stains high-M_r nucleic acids. Finally, the gel was destained in ddH_2O for 10 min. Protein bands possessing ribonucleolytic activity appear clear in a dark purple background.

Assays of ribonuclease inhibitor binding. The fluorescence of fluorescein-labeled A19C/G88R RNase A (fluorescein~RNase A) decreases by ~15% upon binding to porcine RI {Abel, 2002 #1517}. The affinity of G85R/G86R ANG for RI was determined by a competition assay in which G85R/G86R ANG was allowed to bind to RI in the presence of fluorescein~RNase A {Abel, 2002 #1517}. Briefly, G85R/G86R ANG (1 nM – 2 μM) and fluorescein~RNase A (50 nM) were incubated in 2.0 ml of PBS for 30 min at 23°C. The fluorescence intensity (excitation at 491 nm; emission at 511 nm) was measured before and after addition of porcine RI (50 nM). Values of K_d for the complex βween G85R/G86R RNase A and RI were determined as described previously {Abel, 2002 #1517}.

Cell Culture. Human umbilical vein endothelial (HUVE) cells were isolated from fresh cords by an adaptation of the method described by Minick and coworkers (Jaffee *et al.* 1973). Cells were cultured in endothelial basal medium-2 (EBM-2) containing endothelial growth medium (EGM) BulletKit supplements (Clonetics, San Diego, CA) and maintained at

37°C in a humidified atmosphere containing 5% CO_2(g). Experiments were performed with HUVE cells from passage 3 to 6.

Nuclear translocation assay. Fluorescein-labeled ANG was prepared by reaction of the fluorescein succinimidyl ester (Pan Vera, Madison, WI) according to the manufacturer's protocol. HUVE cells were seeded on coverslips (5 x 10^3 cells/cm^2) in the wells of a 6-well culture plate and cultured in the EGM for 24 h. Cells were washed three times with prewarmed EBM-2 and incubated with fluorescein-labeled ANG or G85R/G86R ANG (1 μg/ml) at 37 °C for 1 h. After incubation, cells were washed five times with PBS at 4 °C, and fixed with absolute methanol at -20 °C for 10 min. Cells were viewed with a confocal laser scanning microscope (Carl Zeiss LSM 510).

HUVE cell migration assay. The migration of HUVE cells stimulated by ANG or G85R/G86R ANG was determined by using a scratch wound assay. Briefly, HUVE cells were seeded in 6-well culture plates (5 x 10^3 cells/cm^2) and cultured in EGM. After growing to confluency, cells were washed with prewarmed PBS and cultured in EBM-2 supplemented with 1% fetal bovine serum (FBS) for 24 h. The cell monolayer was scraped with a cell scraper to create a cell-free zone, washed three times with PBS, and incubated with ANG or G85R/G86R ANG (0–1000 ng/ml) in EBM-2 containing 1% FBS. After a 24-h incubation, HUVE cell migration was quantified by measuring the width of the cell free zone (distance βween the edges of the injured monolayer) with a Leica DM IRB real-time inverted microscope.

Rabbit cornea micropocket assay. A hydrogel pellet containing 10 _g of ANG or G85R/G86R ANG was implanted in the micropocket located in the transparent corneal stroma of New Zealand white rabbit eyes. In a blind experiment, the rabbit eyes were

examined daily under slit lamp biomicroscopy by two observers. Pictures of corneal neovascularization were taken with zoom photographic slit lamp (model SM-50F; Takagi®, Nakano, Japan). Corneal neovascularization was measured directly from slides using an image analyzer consisting of a CCD camera (SONY® CCD TR-900, Japan) coupled with a digital analyzer system (Optima® version 5.1.1) on an IBM compatible computer. Angiogenic activity was defined as the number of newly developed vessels multiplied by the length of vessels from the limbus and was measured on postoperative days 3, 7, 10, and 14. Length values were scored according to the following scale: zero for vessels < 0.3 mm; 1 for 0.3 mm – 0.6 mm; 2 for 0.7 mm – 0.9 mm; and 3 for > 1.0 mm. In the case of a vessel that branched into several vessels, the longest vessel was selected as a representative score. The scores of two observers were summed, and the mean was used as the final score.

3.4 Results

Design of RI-evasive ANG. The 3-dimensional structure of the RI·ANG complex demonstrates high complementarity βween the loop formed by residues 84–89 of ANG and human RI (Papageorgiou *et al.* 1997). In particular, Gly 85 and Gly 86 reside in a pocket formed by Trp 263, Trp 261, Ser 289, and Trp 314. The tight packing of these ANG residues closely resembles the interaction of Gly 88 in RNase A with porcine RI (Kobe and Deisenhofer 1995). We introduced Arg residues at positions 85 and 86 of ANG to disrupt RI binding to ANG. The peptide loop containing residues 85 and 86 is distant from the enzymeic active site and, therefore, should not affect the catalytic activity of ANG.

Production of ribonucleases and zymogram electrophoresis. Ribonucleases were produced in *E. coli* with yields of ≥ 40 mg of purified enzyme per liter of culture. Purified enzymes appeared as a single band after SDS-PAGE (data not shown). ANG and G85R/G86R ANG migrated as a single band when subjected to zymogram electrophoresis (Fig. 2). This technique, which can detect as little as 1 pg of RNase A, effectively resolves RNase A and ANG and is an extremely sensitive assay for detecting low levels of RNase A contamination in preparations of ANG (Bravo *et al.* 1994). The presence of a single band for both ANG and G85R/G86R ANG indicates that the proteins used in this study are free from contaminating ribonucleolytic activity.

Assays of ribonucleolytic activity. The values of k_{cat}/K_m for RNase A, G88R RNase A, ANG, and G85R/G86R ANG are listed in Table 1. The k_{cat}/K_m values for ANG and G85R/G86R ANG are indistinguishable, indicating that ribonucleolytic activity of ANG is unaffected by the substitutions.

Assays of ribonuclease inhibitor binding. The values of K_d for complexes of RI with

RNase A, G88R RNase A, ANG, or G85R/G86R ANG are listed in Table 1. The K_d for the complex of RI with G85R/G86R ANG is 5.0 nM, which is ~10–fold higher than that of G88R RNase A (Vicentini *et al.* 1990) and six orders of magnitude higher that of ANG (Lee *et al.* 1989). The K_d values were used to calculate the change in the free energy of association ($\Delta\Delta G$) for RI with each of the ribonucleases. These $\Delta\Delta G$ values are listed in Table 1.

Assays of nuclear translocation. HUVE cells incubated with fluorescein-labeled ANG or G85R/G86R ANG exhibit strong nuclear staining (Fig. 3) and no detectible cytoplasmic staining, indicating that nuclear translocation is not compromised in G85R/G86R ANG.

Assays of HUVE cell migrations. Both ANG and G85R/G86R ANG induce HUVE cell migration in a dose-dependent manner (Fig. 4). The response to both proteins is nearly identical at high protein concentrations (≥500 ng/mL). G85R/G86R ANG, however, stimulates cell migration more efficiently than does ANG at low protein concentrations (≤250 ng/mL).

Assays of angiogenesis in rabbit cornea. Neovascularization of rabbit cornea was stimulated by ANG and G85R/G86R ANG (Fig. 5). Rabbit eyes implanted with a hydrogel packet containing G85R/G86R ANG not only generated more blood vessels, but also demonstrated more rapid blood vessel growth than did eyes implanted with ANG.

3.5 Discussion

The widely accepted mechanism for ANG-induced neovascularization involves three primary steps; (1) binding to a protein receptor present on the surface of endothelial cells and smooth muscle (Hu *et al*, 1997), (2) endocytosis and nuclear translocation (Moroianu and Riordan 1994), and (3) transcriptional activation of rRNA genes (Xu *et al.* 2002). A role for RI in ANG-induced angiogenesis has largely been dismissed despite the remarkably tight complex formed by the two proteins. Numerous studies have identified RI as the primary determinant of ribonuclease cytotoxicity, acting as an intracellular sentry against invading ribonucleases (Haigis *et al.*, 2003; Haigis *et al*, 2002). Yet, a role for RI in normal biological activities has yet to be established. We hypothesized that the complex formed by RI and ANG serves to regulate the biological activity of ANG. Our goals in this study are two-fold: (1) to identify a biological role for RI, and (2) to shed light on the mechanism of ANG-induced cell proliferation.

The most widely used tool for investigating angiogenesis is the chick chorioallantoic membrane (CAM) assay (Riordan 2001). Although ANG effectively stimulates neovascularization in the CAM assay, avian species do not possess a homolog to RI. As a result, many investigators could have overlooked a role for RI in ANG-induced angiogenesis. We assayed angiogenic activity in human endothelial cells (*in vitro*) and rabbit eyes (*in vivo*) to search for such a role.

G85R/G86R ANG proved to be an excellent tool for investigating the role of RI in angiogenesis. Neither its catalytic activity nor its nuclear localization was compromised by the two substitutions. The drastic increase in K_d exhibited by G85R/G86R ANG is nearly two orders of magnitude greater than the change in K_d measured for an analogous variant, G88R

RNase A. Therefore, the observed increase in the biological activity of G85R/G86R ANG *in vitro* and *in vivo* can be attributed to diminished interaction with RI.

Our results are consistent with several mechanisms of ANG regulation by RI. Although RI is not known to be present in the nucleus, its translocation there, as free RI or complexed with ANG, would provide a tight mode of regulation by inhibiting the ribonucleolytic activity of ANG. More likely, is a scenario in which ANG enters the cytosol, where it encounters RI. In this mode of regulation, RI could simply sequester ANG in the cytosol or target ANG for degradation. In turn, modulation of cytosolic RI levels could have profound effects on ANG availability and activity.

A major role for RI is to protect cellular RNA from invading ribonucleases (Haigis *et al.*, 2003). Still, ANG possesses ≥100-fold lower catalytic efficiency than do its homologs with cytotoxic activity. Moreover, the IC_{50} values for cytotoxic ribonucleases are $\geq 10^2$-fold higher than the concentration of ANG required to induce cell proliferation *in vitro*. Thus, a primary role for RI as a cytosolic sentry against invading ANG seems unlikely.

Conclusions. We have revealed a role for RI in ANG-induced angiogenesis. We have created a variant of ANG that evades RI while maintaining its ribonucleolytic activity and nuclear localization. This RI-evasive variant of ANG induces endothelial cell proliferation more efficiently than does ANG both *in vitro* and *in vivo*. This finding provides the first direct evidence that ANG and RI interact in normal biological processes and demonstrates that RI serves to regulate the activity of ANG.

Table 1

Properties of RNase A, ANG, and variants

Ribonuclease	k_{cat}/K_m[a] ($10^6 M^{-1}s^{-1}$)	K_d[b] (nM)	$\Delta\Delta G$[b] (kcal/mol)
ANG	78 ± 12	0.71 x 10^{-7}[c]	0.0
G85R/G86R ANG	73 ± 6	5.0 ± 1	8.9
RNase A	2.1 ± 0.4 x 10^7	59 x 10^{-6}[d]	0.0
G88R RNase A	0.5 ± 0.3 x 10^7	0.57 ± 0.05	5.3

[a]Values of k_{cat}/K_m (±SE) are for catalysis of 6-FAM~dArUdAdA~6-TAMRA cleavage at pH 6.0 and 23 °C.

[b]Values of K_d (±SE) and $\Delta\Delta G = RT\ln(K_d^{variant}/K_d^{wild\text{-}type})$ are for the complex with porcine RI at 23 °C.

[c]Ref (Lee *et al.* 1989; Lee *et al.* 1989).

[d]Ref (Vicentini *et al.* 1990).

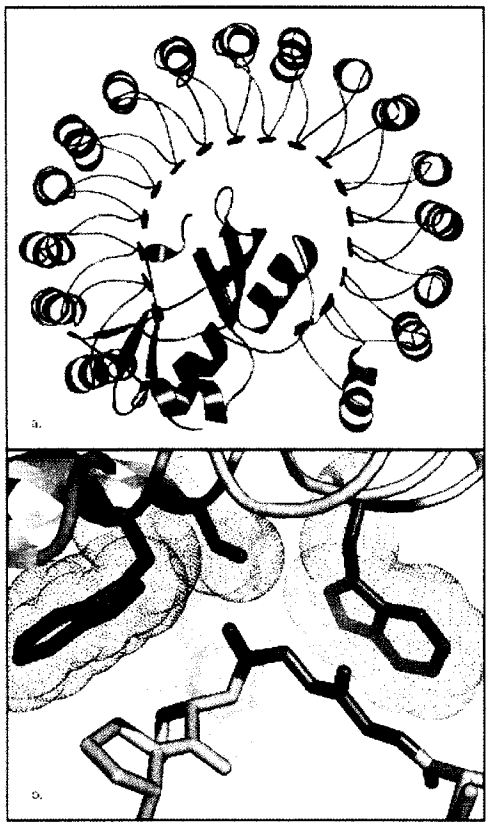

Figure 3.1 Molecular interactions βween human RI (blue) and ANG (rose). Images were created using coordinates from the Protein Data Bank entry 1A4Y and the program PyMOL. (A) Ribbon diagram of the three-dimensional structure of the RI·ANG complex. (B) Contacts βween human RI and residues 85 and 86 of ANG.

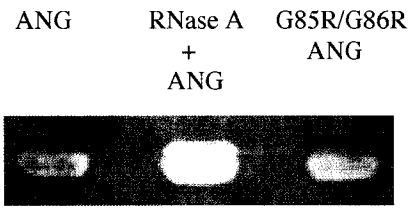

Figure 3.2 Zymogram electrophoresis of ANG and G85R/G86R ANG. Lane 1, ANG (8 μg); lane 2, ANG (8 μg) and RNase A (0.25 ng); lane 3, G85R/G86R ANG (8 μg).

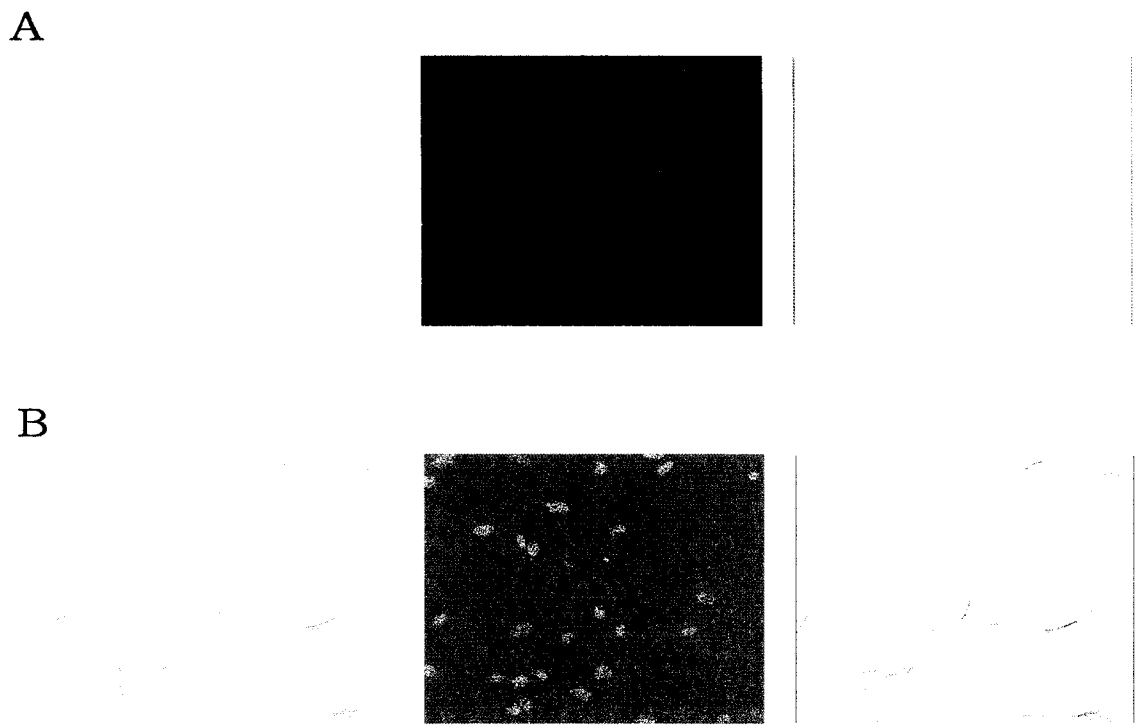

Figure 3.3 Nuclear translocation of ANG (A) and G85R/G86R ANG (B) in HUVE cells *in vitro*. HUVE cells were incubated with 1 μg/ml of fluorescein-labeled ANG (A) or G85R/G86R ANG (B) for 30 min. Localization of the fluorescein-labeled protein was visualized with a confocal laser scanning microscope (Carl Zeiss LSM 510). Left panel, transmission; middle, fluorescein fluorescence; right, merged image.

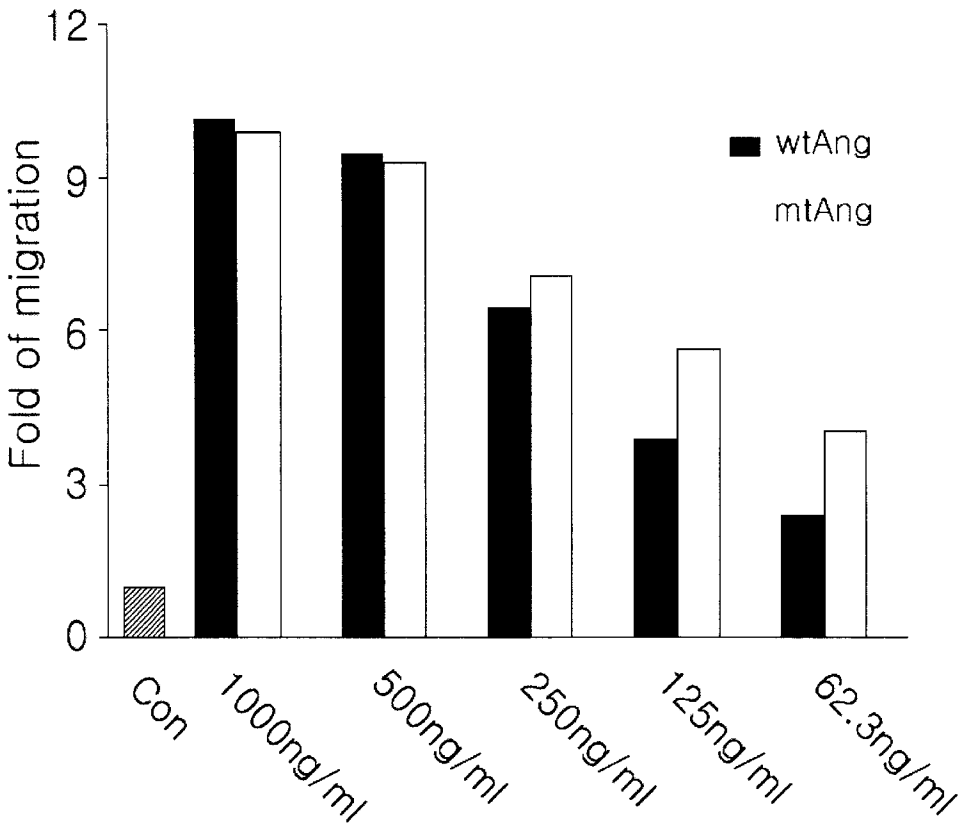

Figure 3.4 Wound healing migration of HUVE cells induced by ANG (solid bars) or G85R/G86R ANG (shaded bars). HUVE cells were plated in 6-well dish, and cell migration was quantified by the scratch wound assay.

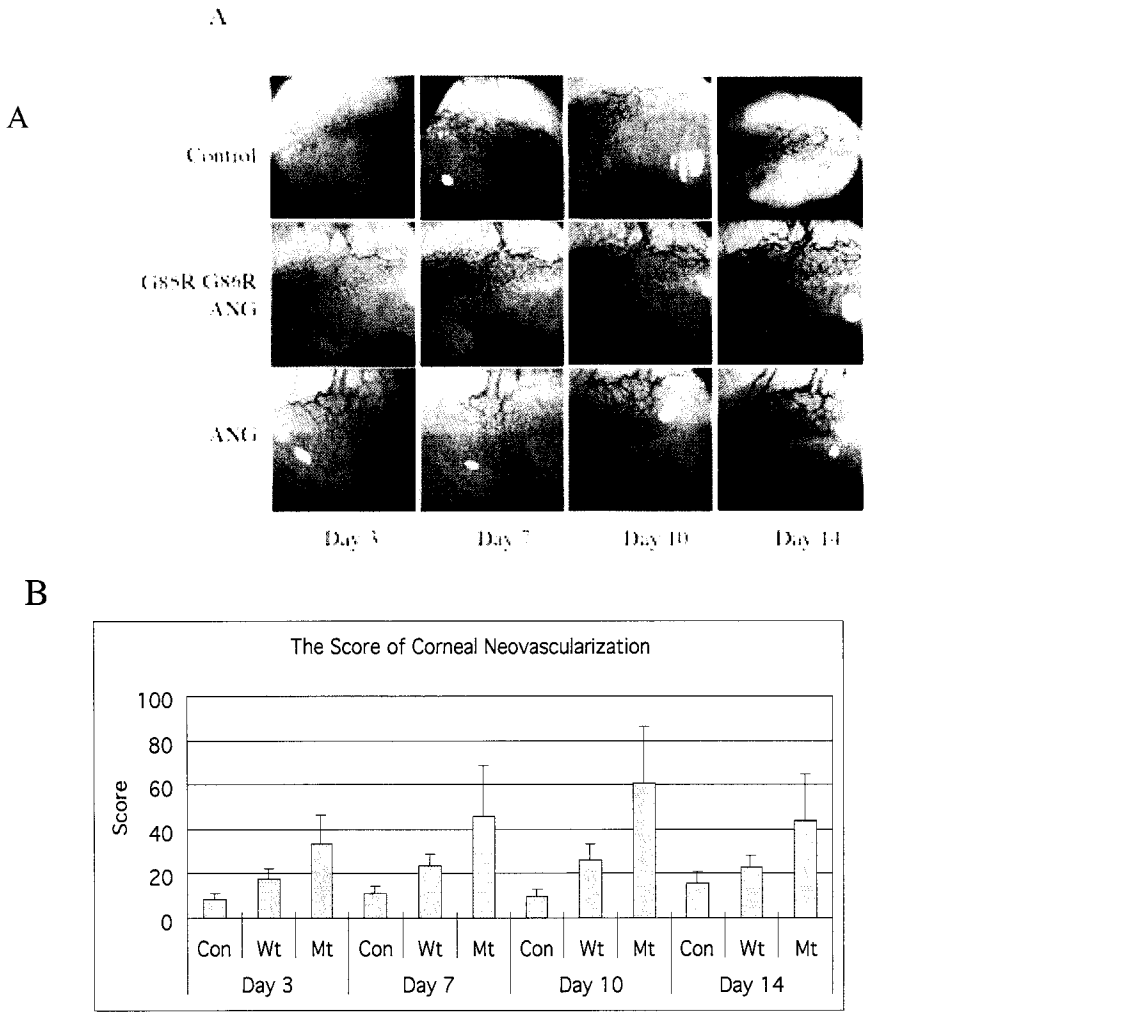

Figure 3.5 Induction of angiogenesis in rabbit cornea *in vivo* by ANG or G85R/G86R ANG. (A) Slit lamp photographs of rabbit corneas 3, 7, 10, and 14 days after implantation with ANG or G85R/G86R ANG. (B) The score of corneal neovascularization.

Chapter Four

Effects of Ribonuclease Inhibitor Silencing on Ribonuclease Toxicity in Human Tumor Cells

4.1 Abstract

The mammalian ribonuclease inhibitor (RI) is an abundant cytoplasmic protein and a potent inhibitor of ribonucleases from the bovine pancreatic ribonuclease (RNase A) superfamily. Amphibian homologs of RNase A and engineered variants of mammalian ribonucleases that evade RI are toxic to tumor cells. The toxicity of a ribonuclease correlates with the magnitude of its catalytic activity in the presence of RI. Mounting evidence suggests that ribonuclease toxicity is highly dependent on internalization as determined by the net positive charge of the protein. Here, we report the effects of RI silencing on the toxicity of ribonucleases in four tumor-derived cell lines. We demonstrate that native levels of RI are necessary to protect some cell lines but appear to play little, if any, role in others. The presence of a protein transduction domain (PTD) loosely correlates with ribonuclease toxicity in some cell lines and can be sufficient to overwhelm RI regardless of its intracellular concentration. In conclusion, the cytotoxic activity of ribonucleases is limited by RI in some but not all human tumor cell lines.

4.2 Introduction

The cytosolic ribonuclease inhibitor (RI) is ubiquitous in mammalian cells, having been detected in all cell types tested (Lee and Vallee 1993; Hofsteenge 1997; Dickson *et al.* 2005). RI binds tightly to the active site of bovine pancreatic ribonuclease (RNase A) as well as other mammalian members of the RNase A superfamily (Lee *et al.* 1989; Vicentini *et al.* 1990). Binding to RI inhibits ribonuclease catalytic activity *in vitro*, though the precise role of RI *in vivo* has not been defined.

Onconase (ONC) and other amphibian homologs of RNase A do not bind to RI and, thus, degrade RNA in its presence. These amphibian ribonucleases demonstrate potent toxicity towards tumor cells. Engineered variants of RNase A and human pancreatic ribonuclease (RNase 1) that evade RI also possess cytotoxic activity (Leland *et al*, 2001; Leland *et al*, 1998; Haigis *et al*, 2002; Rutkoski *et al*, 2005). The most toxic known variant, D38R/R39D/N67R/G88R RNase A, is slightly more toxic to a lymphocitic T-cell line than is ONC (Rutkoski *et al.* 2005). Overexpression of RI in cultured tumor cell lines confers protection against G88R RNase A, a toxic variant of RNase A that maintains diminished but measurable affinity for RI (Haigis *et al*, 2003). These observations indicate that RI is a primary determinant of ribonuclease toxicity. The cytotoxicity correlates strongly with the catalytic activity of a ribonuclease in the presence of RI (Bretscher *et al.* 2000; Dickson *et al.* 2003; Rutkoski *et al.* 2005).

RI evasion is an essential characteristic of a toxic ribonuclease, but it is not the only property that defines ribonuclease toxicity. The net positive charge of a ribonuclease also correlates with toxic activity, but the precise contribution this physical characteristic is

difficult to discern. G88R RNase A possessing a cationic N-terminal protein transduction domain (PTD) composed of 9 arginine residues (R9) demonstrates a 3-fold decrease in its IC_{50} value (Fuchs and Raines 2005). Cationization of RNase A and human pancreatic ribonuclease (RNase 1) with ethylenediamine endows both proteins with cytotoxic activity but also disrupts binding to RI (Futami *et al.* 2001). Similarly, site-directed mutations intended to disrupt an RI–ribonuclease complex often have the secondary effect of increasing the charge of the enzyme (Leland *et al.* 1998). Nonetheless, increasing the charge of a ribonuclease has not been demonstrated to be sufficient to generate a toxic protein.

Here, we employ RNA interference (RNAi) to silence cytosolic RI, thus severely curtailing the protection afforded against an invading ribonuclease. To determine the extent to which RI evasion is a primary determinant of ribonuclease toxicity, we examined the effects of RI silencing in four human cell lines. Cells were exposed to both RI-evasive (toxic) and and non-evasive (non-toxic) ribonucleases under conditions in which cells contained normal or suppressed levels of RI. The data herein demonstrate that ribonuclease toxicity is determined as much by cell-specific characteristics that define ribonuclease internalization and susceptibility to RNA damage as biochemical properties such as RI evasion and net charge of the protein.

4.3 Materials and Methods

Materials. K-562, HeLa, Du-145, and Hep-3b cells were from the American Type Culture Collection (Manasas, VA). Transfection reagents, cell culture medium, and supplements were from Invitrogen (Carlsbad, CA). GeneEraser™ shRNA Mammalian Expression Vector System was from Stratagene (La Jolla, CA). Oligonucleotides encoding shRNAs were synthesized by Integrated DNA Technologies (Coralville, IA). Enzymes for cloning were from Promega (Madison, WI).

Chicken IgY antibodies to human RI and goat anti-chicken secondary antibodies were produced by Genetel (Madison, WI). Rabbit anti-actin primary antibody and goat anti-rabbit secondary antibody were from Santa Cruz Biotech (Santa Cruz, CA). Other immunoblotting reagents including HyBond ECL nitrocellulose membrane, ECL detection reagents, and ECL film were from Amersham Biosciences (Piscataway, NJ). [*methyl*-^{3}H]Thymidine was from Perkin Elmer Life Sciences (Boston, MA). All other chemicals and biochemicals were of reagent grade or βter and were used without further purification.

Analytical Instruments. Ultraviolet and visible absorption was measured with a Cary Model 50 spectrophotometer (Varian; Sugarland, TX). For assays of cytotoxicity, cells were harvested with a PHD Cell Harvester (Cambridge Technology; Watertown, MA). Radioactivity was measured with a Microβa Trilux 2 Detector System (Perkin Elmer; Boston, MA).

Creation of shRNA vectors. Fifteen shRNA sequences designed to target the human RI gene were cloned into plasmid pGE-1, which directs the expression of shRNAs. Only one of these shRNA expression vectors, modeled after an shRNA described previously by D'Alessio and coworkers (Monti and D'Alessio 2004), resulted in significant suppression of RI in the

four cell lines tested. Cloning of this shRNA to create pGE-DAL is described here. Our shRNA targeted the same sequence in RI but was constructed with a different loop sequence. Briefly, the oligonucleotides,

5′-GAT CCC GGT CCT GTC CAG CAC ACT ACG AAG CTT GGT AGT GTG CTG GAC AGG ACC TTT TTT-3′ and

5′-CTA GAA AAA AAG GTC CTG TCC AGC ACA CTA CCA AGC TTC GTA GTG TGC TGG ACA GGA CCG GG-3′

were cloned into the BamHI and XbaI sites of pGE-1. Each oligonucleotide (1 μg) was diluted in 50 μl of 10 mM Tris-HCl buffer pH 8.0, containing NaCl (50 mM) and EDTA (0.1 mM). The oligonucleotide mixture was heated to 93°C for 3 min and then cooled slowly to room temperature. The duplex DNA was ligated into the BamHI and XbaI sites of pGE-1 using the LigaFast kit (Promega, Madison, WI) as directed by the manufacturer. Clones containing the shRNA inserts were confirmed by restriction digest and sequence analysis.

Cell Culture. Du-145 and Hep-3b cells were grown in MEM with Earle's salts, L-glutamine (2 mM), non-essential amino acids (0.1 mM), and sodium pyruvate (1 mM). K-562 cells were grown in RPMI medium 1640; HeLa cells were grown in DMEM. All culture medium was supplemented with fetal bovine serum (10% v/v), penicillin (100 U/ml), and streptomycin (100 μg/ml). Cultures were maintained in a humidified incubator at 37°C containing 5% CO_2(g).

Transfection of Human Cells. Transfection of K-562, HeLa, Du-145, and Hep-3b cells was carried out in 6-well dishes using Lipofectamine 2000 and Opti-MEM medium (Invitrogen, Carlsbad, CA). Briefly, cells were seeded at 0.5 x 10^6 cells/well and incubated at 37°C for 6–12 hours in normal growth medium. DNA-Lipofectamine 2000 complexes were

formed with 4–7 μg DNA and 4–10 μl of Lipofectamine 2000 as directed by the manufacturer. Cells were washed with warm serum-free Opti-MEM prior to adding DNA–lipid complexes. Cells were incubated with DNA–lipid complexes for 4–6 h, after which the medium was replaced with Opti-MEM containing FBS (10% v/v). Cells were incubated for 44 h before passage to 75 cm^2 flasks containing 600 μg/ml Geneticin. Stably transfected cells were maintained and propagated in normal growth medium containing Geneticin (600 μg/ml).

Production of Ribonucleases. All ribonucleases used in this study were purified as describe previously (delCardayré *et al.* 1995). Protein concentrations were determined by UV spectroscopy using $\varepsilon = 0.72$ mL mg^{-1} cm^{-1} at 280 nm for RNase A and its variants and $\varepsilon = 0.87$ mL mg^{-1} cm^{-1} at 280 nm for ONC. Prior to cytotoxicity assays, ribonucleases were dialyzed extensively versus phosphate–buffered saline (PBS).

Assays of cytotoxicity. The cytotoxicity of ribonucleases was determined by measuring the incorporation of [*methyl*-^{3}H]thymidine into the DNA of stably transfected human cell lines. Briefly, cells were seeded in 96-well plate in 100 μl of normal growth medium at a density of 5000 cells/well. Ribonucleases in PBS (5 μL) were incubated with cells for 44 h at 37 °C, followed by incubation with [*methyl*-^{3}H]thymidine (0.4 μCi/well) for 4 h. Cells were harvested onto a glass fiber filter and ^{3}H incorporated into each sample was counted. Cells incubated with PBS alone were used to determine 100% ^{3}H incorporation. IC_{50} values were determined by fitting the data to the equation $S = 100 \times IC_{50}/(IC_{50} + [\text{ribonuclease}])$, where *S* is the percentage of [*methyl*-^{3}H]thymidine incorporation after a 48-h incubation with a ribonuclease.

Immunoblotting. The soluble protein fraction of stably transfected cells was prepared

from a wet cell pellet using MPER lysis solution containing HALT protease inhibitor cocktail (Pierce Biotech, Rockford, IL). Briefly, cells from a 75–cm^2 flask were harvested and washed 3× with PBS. The cell pellet was resuspended in MPER (10 μl/10^6 cells) and incubated on ice for 30 min. Cells were passed 5× through a 24–G syringe, and cell debris was pelleted by centrifugation at 15,000 g for 10 min. Protein extracts were stored at -80 °C until use.

Lysates from stably transfected cells (3 μg) were subjected to SDS–PAGE on a 4–15% Tris–HCl Ready Gel (BioRad, Hercules, CA) along with recombinant human RI (1–100 ng) and Precision Plus prestained MW standards (BioRad, Hercules, CA). Proteins were transferred to HyBond ECL nitrocellulose and then blocked overnight in TBS-T [20 mM Tris–HCl buffer, pH 7.5, containing NaCl (0.137 mM) and Tween 20 (0.2% w/v)] containing non-fat dry milk (4% w/v). Blots were incubated with anti-hRI IgY (1:3000 dilution in blocking solution) for 1 h and then washed 3× with TBS-T (15 mL). Blots were then incubated with a horseradish peroxidase (HRP) -conjugated goat anti-chicken antibody (1:5000 dilution in blocking solution) for 1 h, and then washed (4×) with TBS-T (15 mL). RI was visualized using ECL–detection reagents and exposure to ECL film.

The results of the two blots were compared directly because they were run simultaneously and exposed to the same washing and blotting solutions. Bands were analyzed from a scanned film image using ImageQuantTL (Sunnyvale, CA). Briefly, bands were selected using ImageQuantTL by drawing a rectangle with a slightly greater area than the largest band. The intensity of each band in the RI standard curve was calculated using ImageQuantTL. The values for RI bands in the cell lysate were determined by the same method and were compared to those obtained from the standard curve.

To insure equal loading of cell lysate samples, the blot was stripped and re-probed for actin. Briefly, blots were incubated with 30 mL Restore Western Blot Stripping Buffer (Pierce Biotechnology, Rockford, IL) for 30 min, and then washed briefly with 20 mL TBS-T. Blots were incubated with primary and secondary antibodies, visualized, and analyzed as described above. Rabbit anti-actin and HRP-conjugated goat anti rabbit antibodies were diluted 1:5000 and 1:10,000, respectively, in blocking solution.

4.4 Results

Suppression of cytosolic RI. We constructed 15 distinct shRNA vectors designed to target the RI gene. Of the 15 target sequences, 14 were unique target sequences designed using shRNA algorithms from Invitrogen and Greg Hannon's laboratory (Cold Spring Harbor Laboratories, NY). One shRNA, pGE-DAL, was modeled after a previously reported shRNA sequence (Monti and D'Alessio 2004). None of the 14 unique sequences were capable of significantly reducing RI expression. Thus, RI suppression was achieved using pGE-DAL in all data described below.

The extent of RI suppression in stably transfected mammalian cells was determined by immunoblotting. Analysis of the soluble protein fraction of cells transfected with a negative control vector, pGE-Neg, or pGE-DAL indicated that suppression of RI is not complete; faint bands corresponding to low levels of RI expression are present in all four transfected cell lines (Fig 1B). After normalizing the intensity of RI bands from lysate samples according to the intensity of an actin loading control, the percent knockdown was determined by comparing the intensity of RI bands from cell lysates against known amounts of RI (Fig 1A). The extent of suppression ranged from 52 to 63% (Fig 1C).

Cytotoxicity. We measured the susceptibility of mammalian cells stably transfected with pGE-NEG or pGE-DAL to RI-evasive and non-evasive ribonucleases. The RI-evasive ribonucleases tested included ONC, which demonstrates no measurable affinity for RI, and two RNase A variants (G88R RNase A and K41R/G88R RNase A), which possess measurable but weak affinity for RI. Non RI-evasive ribonucleases included RNase A, RNase 1, and RNase A–R9. In all cases, the IC_{50} values for ONC were the same in cells expressing pGE-Neg or pGE-DAL (Table 1). The cytotoxicity of all other ribonucleases is described below.

The results of cytotoxicity experiments varied significantly βween the four mammalian cell lines examined in this study. Two cell lines, HeLa and Hep-3b, demonstrated similar trends. Briefly, the IC_{50} values for the RI-evasive variants of RNase A (G88R RNase A and K41R/G88R RNase A) decreased when cytosolic levels of RI were suppressed (Fig 2, Table 1). In addition, the IC_{50} values for RNase A–R9, which does not evade RI, decreases by ~4-fold in cells expressing pGE-DAL, whereas the values for RNase A and RNase 1 remained unchanged.

Surprisingly, Du-145 cells reacted similarly to exogenous ribonucleases regardless of cytosolic RI levels (Table 1). No statistically significant decrease in the IC_{50} values for any ribonuclease, either RI-evasive or non-evasive, was observed in cells transfected with pGE-DAL. Both wild-type RNase A and RNase A–R9 demonstrated measurable and significant toxicity towards DU-145 cells; the IC_{50} values for the two proteins differed by only ~2.5-fold. In addition, G88R RNase A and K41R/G88R RNase A demonstrated similar toxic activity as wild-type RNase A, possessing IC_{50} values that differed from RNase A by less than 20%. Unlike RNase A, wild-type RNase 1 demonstrated no detectible toxicity towards Du-145 cells.

In K-562 cells, only G88R RNase A and K41R/G88R RNase A demonstrate increased cytotoxicity in cells expressing pGE-DAL. All other IC_{50} values were independent of cytosolic RI levels.

In general, the magnitude of change ribonuclease cytoxicity induced by RI suppression was substantial; most IC_{50} values decreased by >75%. These substantial increases in ribonuclease susceptibility were independent of initial IC_{50} values in cells expressing pGE-Neg. For example, the IC_{50} values for G88R RNase A and RNase A–R9 differed by 10-fold in Hep-3b cells expressing pGE-Neg. Yet, both IC_{50} values decreased by ~75% upon RI knock down.

4.5 Discussion

RI is horseshoe-shaped protein composed of 16 consecutive leucine–rich repeats (LRRs) (Kobe and Deisenhofer 1993). The genetic structure of RI mirrors the primary structure of the protein; 7 exons code for 7 discrete LRR pairs (Haigis *et al.* 2002). Pairwise analysis of these exons revealed 50–60% sequence identity (Haigis *et al.* 2002). Despite its highly repetitive sequence with significant sequence identity, RI has proved to be a difficult target for RNAi. In total, we constructed 14 unique shRNA sequences that had little effect on the cytosolic concentration of RI. Only pGE-DAL was capable of drastically altering RI levels. Initial observation of immuno blots indicated that RI knock down was substantial, though not complete. Indeed, quantitative analysis of the blot revealed that RI levels in all four human cell lines were reduced by only 52–66%. These data demonstrate that intracellular RI levels in cells harboring pGE-DAL are sufficient to present a formidable line of defense against invading ribonucleases. IC_{50} values for ribonucleases will only decrease if

the amount of ribonuclease internalized is adequate to saturate and thus overwhelm the remaining RI.

Nonspecific suppression by RNAi has been well documented (Scacheri *et al.* 2003). To demonstrate that the DAL shRNA specifically targets RI and does not affect other proteins that enhance ribonuclease susceptibility, we compared the toxicity of ONC in cells transfected with either pGE-Neg or pGE-DAL. Because ONC does not bind to RI, the IC_{50} values for ONC should remain unchanged in the presence of the DAL shRNA. Indeed, none of the four cell lines examined demonstrated increased sensitivity to ONC when RI was knocked down. Likewise, the IC_{50} values for ONC, G88R RNase A and K41R/G88R RNase A incubated with K-562 cells expressing pGE-NEG are similar to values reported previously for non-transfected K-562 cells (data not shown). Therefore, neither the presence of shRNA molecules nor the specific suppression of RI in a cell confers additional susceptibility to ribonucleases.

For a ribonuclease to be toxic to a cell, it must first gain access to the cytosol. This process involves binding to the cell surface, internalization via an endocytic vesicle, and translocation through a membrane to reach the cytosol (Haigis and Raines 2003). Most ribonuclease molecules that enter a cell are degraded in endocytic vesicles; few make it to the cytosol intact. Thus, internalization is a major determinant of ribonuclease cytotoxicity. Molecules that are more efficient at reaching the cytosol are more toxic. Presumably, PTDs, chemical cationization, and increased charge incurred through site-directed mutagenesis enable ribonucleases to be internalized more efficiently than their wild-type progenitors.

After internalization, a toxic ribonuclease degrades cellular RNA. Presumably, ribonucleases that bind tightly to RI, such as RNase A and RNase 1, must saturate cytosolic

RI before they can elicit toxic effects. Previous studies in normal and tumor-derived cell lines indicate that intracellular RI levels do not correlate with the resistance of cells to ribonucleases (Haigis *et al.* 2002). Here, immunoblots reveal that the concentration of RI in pGE-NEG cell extracts differs by less than 30%. Therefore, variations in ribonuclease resistance βween the four cell types examined here cannot be attributed to differences in cytosolic levels of RI. Rather, ease of internalization or other cell type-specific factors determine the relative susceptibility or resistance to ribonucleases. The experiments described herin have allowed us to scrutinize the role of RI evasion in defining ribonuclease toxicity to provide a clearer picture of the mechanism of ribonuclease cytotoxicity.

HeLa and Hep-3b cells rely on protection by RI, as intracellular levels of RI limit ribonuclease toxicity. Reduction of RI levels in both of these cell types results in a significant decrease in the IC_{50} values of RI-evasive RNase A variants as well as RNase A–R9, which binds tightly to RI but exhibits extremely efficient internalization due to its PTD. G88R RNase A and K41R/G88R RNase A become more toxic to the cell because fewer molecules are hindered by weak interactions with RI. Despite its tight binding to RI, RNase A–R9 is internalized efficiently and is toxic to cells transfected with pGE-NEG. The IC_{50} values decreases in cells possessing pGE-DAL because fewer RNase A–R9 molecules are required to saturate the remaining RI.

The effect of RI silencing in K-562 cells is similar to that in HeLa and Hep-3b cells. The IC_{50} values for G88R RNase A and K41R/G88R RNase A decrease upon suppression of RI. Surprisingly, K-562 cells are susceptible to RNase A–R9, yet the IC_{50} value for RNase A–R9 remains unchanged in pGE-DAL K-562 cells. Possibly, the R9 tag affords exceptional internalization in K-562 cells such that endogenous RI provides little protection at high

concentrations of RNase A–R9.

Du-145 cells are susceptible to RNase A and its variants, yet are not affected by suppression of RI. Surprisingly, the IC_{50} values for RNase A are similar to those for RI-evasive variants of RNase A. Possibly, reduction of cytosolic RI levels in Du-145 cells is insufficient to generate a change in IC_{50} values. Du-145 cells also exhibit higher IC_{50} values for RI-evasive RNase A variants than any other cell line tested. These data indicate that RNase A and its variants do not gain access to the cytosol of Du-145 cells efficiently.

Both RNase 1 and RNase A demonstrated measurable but weak toxicity in some, but not all cell lines. Tranformation of these cell lines with pGE-DAL had no effect on IC_{50} values for either protein. RNase 1 and RNase A share 70% sequence identity (Moore and Stein 1973; Beintema *et al.* 1984), are both highly cationic proteins (pI = 8.6 and 9.4, respectively) (Tanford and Hauenstein 1956; Zhang *et al.* 2003), and are robust catalysts of RNA degradation (Leland *et al.* 2001). Despite shared biochemical properties, RNase A and RNase 1 demonstrate different cytotoxic activities in the cell lines tested.

We have illustrated a complex relationship βween ribonucleases and tumor cells in which internalization, RI evasion, and subsequent RNA degradation are predominantly dictated by cell type. Although RI evasion correlates directly with cytotoxicity in numerous cell lines, decreases in intracellular RI levels do not generate consistent decreases in IC_{50} values. In addition, the net charge of a ribonuclease correlates weakly, if at all, with toxicity. The data presented here indicate that salient features of the mechanism of ribonuclease cytotoxicity, including the mode of internalization, remain to be discovered.

Table 4.1. IC_{50} values of RI-evasive and non-evasive ribonucleases in tumor cell lines with and without RI suppression. Values in bold-face type decrease significantly upon RI suppression.

		IC_{50} values (μM)					
		RI-evasive ribonucleases			**Non-evasive ribonucleases**		
		G88R RNase A	K41R/G88R RNase A	ONC	RNase A	RNase 1	RNase A–R9
K-562	NEG	**4.5 ± 0.6**	**9.22 ± 1**	0.49 ± 0.07	>200	65 ± 8	29 ± 3
	DAL	**0.97 ± 0.09**	**6.28 ± 0.8**	0.51 ± 0.06	>200	66 ± 6	27 ± 3
HeLa	NEG	**67 ± 11**	**>25**	0.90 ± 0.22	>200	44 ± 4	**14 ± 2**
	DAL	**9.7 ± 2**	**8.5 ± 2**	0.75 ± 0.25	>200	37 ± 5	**3.1 ± 0.9**
Du-145	NEG	71 ± 8	51 ± 10	0.18 ± 0.02	65 ± 6	>200	11 ± 2
	DAL	61 ± 7	39 ± 5	0.16 ± 0.02	61 ± 7	>200	8 ± 2
Hep-3b	NEG	**13 ± 2**	**13 ± 2**	0.14 ± 0.03	>200	>200	**112 ± 23**
	DAL	**3.0 ± 0.9**	**1.9 ± 0.9**	0.13 ± 0.03	>200	>200	**31 ± 8**

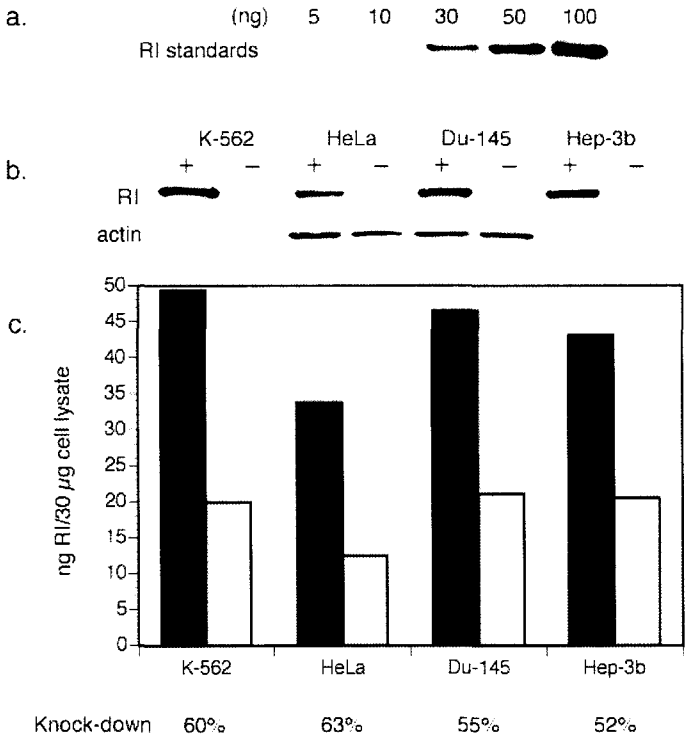

Figure 4.1 Immunoblot analysis of RI suppression in human tumor cell lines: (a) RI standards. (b) Cell lysate (30 μg) transfected with pGE-NEG (-) or pGE-DAL (+) probed with anti-RI or anti-actin antibodies. (c) Amount of RI present in transfected cells determined by comparing the intensity of RI bands from cell lysates against a standard curve generated from RI standards. Analysis was performed using ImageQuantTL as described in Methods.

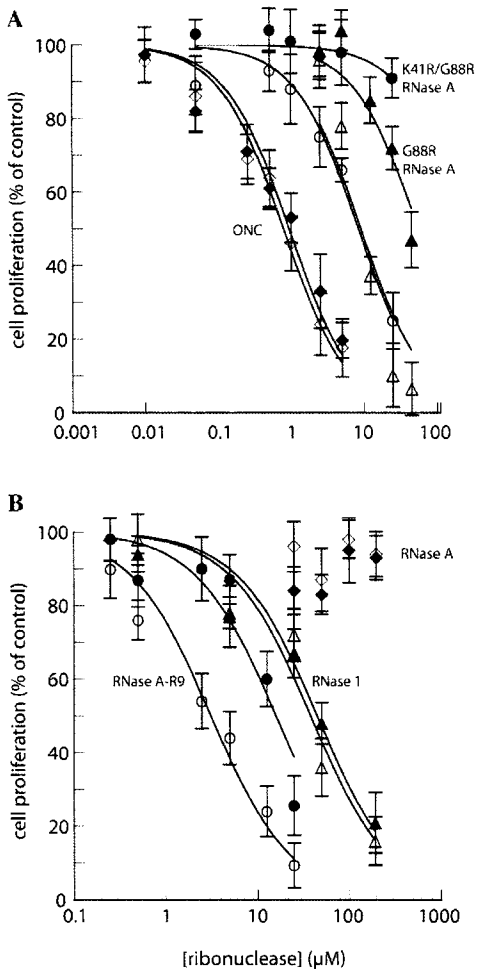

Figure 4.2 Effect of ribonucleases on the proliferation of HeLa cells transfected with pGE-NEG (closed symbols) or pGE-DAL (open symbols). (a) RI-evasive ribonucleases: G88R RNase A (triangles), K41R/G88R RNase A (circles), or ONC (diamonds). (b) Non-evasive ribonucleases: RNase 1 (triangles), RNase A (diamonds), and RNase A–R9 (circles).

Appendix I

Production of a Cysteine-Free Ribonuclease Inhibitor

AI.1 Introduction

Porcine and human RI contain 30 and 32 cysteines, respectively, which must be reduced for the protein to be functional (Hofsteenge *et al.* 1988; Lee *et al.* 1988). Oxidation of RI is a highly cooperative process; oxidation of only a few cysteines changes the conformation of the protein and renders the remaining thiols extremely reactive (Fominaya and Hofsteeenge, 1992). An oxidation-resistant RI could serve as a useful laboratory reagent and could be a useful tool in investigating RI-RNase interactions. The goal of this work was to create a cysteine-free porcine RI (pRI) in which all of the cysteine residues are replaced with alanine.

AI.2 Materials and Methods

Mutagenesis of pRI was performed on the plasmid pTrpRI6.1 (Klink and Raines, 2001). Primers coding for Cys to Ala mutations were produced by IDT (Coralville, IA). Mutagenesis was performed using the QuickChange Multi kit from Stratagene (La Jolla, CA) according to the manufacturers instructions. As many as 6 mutations were attempted in a single round of mutagenesis; 6 rounds of mutagenesis were required to alter all 30 Cys to Ala. Mutant pRI (pTrpRI6.1-Ala) clones were screened by sequence analysis.

The binding activity Ala-pRI compared to pRI was determined from a lysate of cells overexpressing RI. Briefly, *E. coli* TOPP3 cells were transformed with pTrpRI6.1 or pTrpRI6.1-Ala and grown in LB to mid-log phase (OD_{600} = 1.0), after which, cells were harvested and resuspended in M9 minimal media (Klink and Raines, 2001). Cells were grown at in minimal media at 16°C for 12 hours and then harvested. Cells were lysed by sonication and cell debris was removed by centrifugation at 40,000 ×g. The supernatant of this

procedure is the cell lysate used to assess the activity of Ala-pRI.

AI.3 Results

Cell lysate of *E. coli* expressing pRI or Ala-pRI was analyzed by SDS-PAGE. Induction of pRI and Ala-pRI was detectible, and comparable to previously reported levels of expression (Klink and Raines, 2001). The relative amount of soluble and insoluble protein in each sample was not determined.

The ability of pRI or Ala-pRI to bind to RNases was determined by its ability to inhibit the catalytic activty of RNase A. Assays were carried out using the fluorogenic stubstrate, IDT2, in 100 mM MES buffer, pH 6.0, containing 100 mM NaCl and 1 mM DTT. Crude cell lysate of cells expressing pRI was diluted 1:100 in reaction buffer; addition of only 10 μL of the diluted lysate completely abolished ribonucleolytic activity. Conversely, addition of 1 - 200 μL of undiluted Ala-pRI lysate did not inhibit RNase A, but slightly increased the ribonucleolytic activity.

The inability of Ala-pRI to inhibit RNase A could be a result of decreased affinity or compromised structural stability. No attempt was made to evaluate the ability of Ala-pRI to fold in vivo or in vitro, and it was concluded that Ala-pRI was not sufficiently functional for subsequent investigations.

Appendix II

Ribonuclease Binding to the Cell Surface

AII.1 Introduction

Binding of RNase A and its homologs to the suface of mammalian cells facilitates their entry into the cytosol (Haigis and Raines, 2002). The specific interactions of ribonucleases with molecules displayed on the surface of cells have not been described. The purpose of this work was to measure the affinity of RNase A and Onconase ™ for the surface cultured tumor cells in order to identify specific interactions βween ribonucleases and cell-surface residues.

AII.2 Materials and Methods

K-562, HeLa, and LacZ-9L glioma cells were obtained from ATCC (Manasas, VA) and were cultured according to ATCC instructions in RPMI (for K-562) or DMEM (for HeLa and LacZ-9L). All media contained FBS (10% v/v), penicillin (100 units/mL), and streptomycin (100 μg/mL). A19C RNase A and D16C ONC were produced and labeled with 5-iodoacetamidofluorescein (5-IAF) as described previously (Haigis and Raines, 2002). Ribonuclease binding to the surface of cells was assayed by flow cytometry. Briefly, cells were harvested, washed in ice-cold media, and resuspended at a density of 1 x 10^6 cells/mL. Cells were maintained on ice for the duration of the experiment. Fluorescently labeled ribonucleases were added to the suspension of cells and incubated on ice for >30 min. In some cases, the cells were washed 3x with ice-cold PBS prior to flow cytometry.

AII.3 Results

In all conditions tested, both RNase A and ONC demonstrated non-specific binding to the surface of cultured mammalian tumor cells. The fluorescence intensity associated with

cells increased linearly with the concentration of protein added to the media (Fig A1). Cells treated with trypsin or neuraminidase (sialidase) did not demonstrate decreased ribonuclease binding. In addition, the addition of colominic acid (polysialic acid) at 13.3 mg/ml, ribonuclease inhibitors (5'-AMP and 3'-UMP at 35 and 400 μM, respectively), polylysine at 5 mg/ml, heparin sulfate at 3.3 mg/ml, or NaCl at twice the concentration of the media (400 mM total) did not cause a detectible change in ribonuclease binding. Finally, ribonuclease binding was not affected by the presence of FCS in the media.

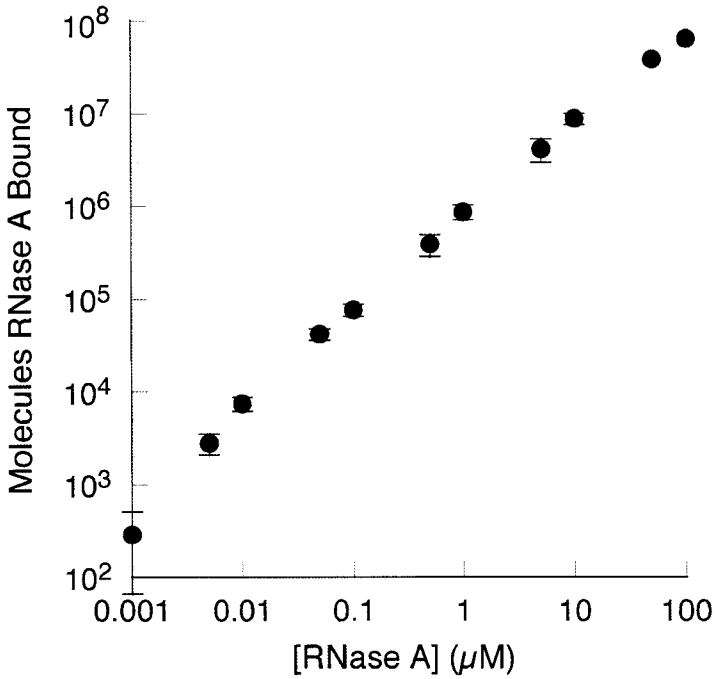

Figure AII.1 Binding of fluorescein-labeled RNase A to K-562 cells. Cells were incubated with labeled RNase A for 30 min on ice. Fluorescence was measured by flow cytometry. The number of RNase A molecules bound was determined by comparing the florescence of cell with that of fluorescein-labeled beads as described in Methods.

References

Abel, R. A., M. C. Haigis, C. Park and R. T. Raines (2001). Fluorescence assay for the binding of ribonuclease A to its cytosolic inhibitor protein. *Anal Biochem* **360**, 100-107.

Allen, D. W. and J. H. Jandl (1961). Oxidative hemolysis and precipitation of hemoglobin. II. Role of thiols in oxidant drug action. *J. Clin. Invest.* **40**, 454-475.

Ardelt, W., S. M. Mikulski and K. Shogen (1991). Amino acid sequence of an anti-tumor protein from *Rana pipiens* oocytes and early embryos. *J. Biol. Chem.* **266**, 245-251.

Beintema, J. J., P. Wietzes, J. L. Weickmann and D. G. Glitz (1984). The amino acid sequence of human pancreatic ribonuclease. *Anal. Biochem.* **136,** 48-64.

Blackburn, P. (1979). Ribonuclease inhibitor from human placenta: Rapid purification and assay. *J. Biol. Chem.* **254**, 12484-12487.

Blackburn, P. and B. L. Jailkhan (1979). Ribonuclease inhibitor from human placenta: Interaction with deriviatives of ribonuclease A. *J. Biol. Chem.* **254**, 12488-12493.

Blackburn, P. and S. Moore (1982). Pancreatic ribonuclease. *The Enzymes* XV: 317-433.

Blackburn, P., G. Wilson and S. Moore (1977). Ribonuclease inhibitor from human placenta. Purification and properties. *J. Biol. Chem.* **252**, 5904-5910.

Blázuez, M., J. M. Fominaya and J. Hofsteenge (1996). Oxidation of sulfhydryl groups of ribonuclease inhibitor in epithelial cells is sufficient for its intracellular degradation. *J. Biol. Chem.* **271**, 18638-18642.

Bläser, J., S. Triebel, C. Kopp and H. Tschesche (1993). A highly sensitive immunoenzymometric assay for the determination of angiogenin. *Eur. J. Clin. Chem. Clin. Biochem.* **31**, 513-516.

Boix, E., Y. Wu, V. M. Vasandani, S. K. Saxena, W. Ardelt, J. Ladner and R. J. Youle (1996). Role of the N terminus in RNase A homologues: Differences in catalytic activity, ribonuclease inhibitor interaction and cytotoxicity. *J. Mol. Biol.* **257**, 992-1007.

Botella-Estrada, R., G. Malet, F. Revert, F. Dasi, A. Crespo, O. Sanmartin, C. Guillen and S. F. Alino (2001). Antitumor effect of B16 melanoma cells genetically modified with the angiogenesis inhibitor rnasin. *Cancer Gene Ther.* **8**, 278-284.

Bravo, J., E. Fernández, M. Ribó, R. de Llorens and C. M. Cuchillo (1994). A versatile negative-staining ribonuclease zymogram. *Anal. Biochem.* **219,** 82-86.

Bretscher, L. E., R. L. Abel and R. T. Raines (2000). A ribonuclease A variant with low catalytic activity but high cytotoxicity. *J. Biol. Chem.* **275,** 9893-9896.

Burton, L. E., P. Blackburn and S. Moore (1980). Ribonuclease inhibitor from bovine brain. *Int. J. Peptide Protein Res.* **16**, 359-364.

Burton, L. E. and N. P. Fucci (1982). Ribonuclease inhibitors from the liver of five mammalian species. *Int. J. Peptide Protein Res.* **19**, 372-379.

Cavalli, L., D. Galaverni, P. Pesando, P. G. Bracchi, G. Campanini and G. Maraini (1979). Control of ribonuclease activity in the human lens during aging and cataract formation. *Ophthalmic Res.* **11**, 416-422.

Chen, C.-Z. and R. Shapiro (1997). Site-specific mutagenesis reveals differences in the structural bases for tight binding of RNase inhibitor to angiogenin and RNase A. *Proc. Natl. Acad. Sci. USA* **94**, 1761-1766.

Chen, C. Z. and R. Shapiro (1999). Superadditive and subadditive effects of "hot spot" mutations within the interfaces of placental ribonuclease inhibitor with angiogenin and ribonuclease A. *Biochemistry* **38**, 9273-9285.

Cho, S. and J. G. Joshi (1989). Ribonuclease inhibitor from pig brain: purification, characterization, and direct spectrophotometric assay. *Anal. Biochem.* **176**, 175-181.

Crawford, D., K. Hagerty and B. Beutler (1989). Multiple splice forms of ribonuclease-inhibitor mRNA differ in the 5'- untranslated region. *Gene* **85**, 525-531.

Crick, F. H. C. (1952). Is a-keratin a coiled coil? *Nature* **170**, 882-883.

Cui, X. Y., P. F. Fu, D. N. Pan, Y. Zhao, J. Zhao and B. C. Zhao (2003). The antioxidant effects of ribonuclease inhibitor. *Free Radic. Res.* **37**, 1079-1085.

Darzynkiewicz, Z., S. P. Carter, S. M. Mikulski, W. J. Ardelt and K. Shogen (1988). Cytostatic and cytotoxic effect of Pannon (P-30 Protein), a novel anticancer agent. *Cell Tissue Kinet.* **21**, 169-182.

delCardayré, S. B., M. Ribó, E. M. Yokel, D. J. Quirk, W. J. Rutter and R. T. Raines (1995). Engineering ribonuclease A: Production, purification, and characterization of wild-type enzyme and mutants at Gln11. *Protein Eng.* **8**, 261-273.

Dickson, K. A., C. L. Dahlberg and R. T. Raines (2003). Compensating effects on the cytotoxicity of ribonuclease A variants. *Arch. Biochem. Biophys.* **415** 172-177.

Dickson, K. A., M. C. Haigis and R. T. Raines (2005). Ribonuclease inhibitor: structure and function. *Prog. Nucleic Acid Res. Mol. Biol.* **80**, 349-374.

Dijkstra, J., J. Touw, I. Halsema, M. Gruber and G. Ab (1978). Estradiol-induced synthesis of vitellogenin. *Biochim Biophys Acta.* **521**, 363-373.

Eberhardt, E. S., P. K. Wittmayer, B. M. Templer and R. T. Raines (1996). Contribution of a tyrosine side chain to ribonuclease A catalysis and stability. *Protein Sci.* **5**, 1697-1703.

Ellis, R. J. (2001). Macromolecular crowding: Obvious but unappreciated. *Trends Biochem. Sci.* **26**, 597-604.

Evdokimov, A. G., D. E. Anderson, K. M. Routzahn and D. S. Waugh (2001). Unusual molecular architecture of the Yersinia pestis cytotoxin YopM: A leucine-rich repeat protein with the shortest repeating unit. *J. Mol. Bio.* **312**, 807-821.

Ferreras, M., J. G. Gavilanes, C. Lopéz-Otín and J. M. García-Segura (1995). Thiol-disulfide exchange of ribonuclease inhibitor bound to ribonuclease A. *J. Biol. Chem.* **270**, 28570-28578.

Fett, J. W., D. J. Strydom, R. R. Lobb, E. M. Alderman, J. L. βhune, J. F. Riordan and B. L. Vallee (1985). Isolation and characterization of angiogenin, an angiogenic protein from human carcinoma cells. *Biochemistry* **24**, 5480-5486.

Fominaya, J. M. and J. Hofsteenge (1992). Inactivation of ribonuclease inhibitor by thiol–disulfide exchange. *J. Biol. Chem.* **267**, 24655-24660.

Fuchs, S. M. and R. T. Raines (2005). Polyarginine as a multifunctional fusion tag. *Protein Sci.* **14**, 1538-1544.

Futami, J., T. Maeda, M. Kitazoe, E. Nukui, H. Tada, M. Seno, M. Kosaka and H. Yamada (2001). Preparation of potent cytotoxic ribonucleases by cationization: Enhanced cellular uptake and decreased interaction with ribonuclease inhibitor by chemical modification of carboxyl groups. *Biochemistry* **26**, 7518-7524.

Futami, J., K. Nukui, T. Maeda, M. Kosaka, H. Tada, M. Seno and H. Yamada (2002). Optimum modification for the highest cytotoxicity of cationized ribonuclease. *J. Biochem. (Tokyo)* **132**, 223-228.

Futami, J., Y. Tsushima, Y. Murato, H. Tada, J. Sasaki, M. Seno and H. Yamada (1997). Tissue-specific expression of pancreatic-type RNases and RNase inhibitor in humans. *DNA Cell. Biol.* **16**, 413-419.

G.-F., H., J. F. Riordan and B. L. Vallee (1994). Angiogenin promotes invasiveness of cultured endothelial cells by stimulation of cell-associated proteolytic activities. *Proc. Natl. Acad. Sci. U.S.A.* **94**, 2204-2209.

Garcia, M. A. and R. J. Klebe (1997). Affinity chromatography of RNase inhibitor. *Mol. Biol. Rep.* **24**, 231-233.

Green, N. M. (1975). Avidin. *Adv. Protein Chem.* **29**, 85-133.

Gribnau, A. A., J. G. Schoenmakers, M. van Kraaikamp, M. Hilak and H. Bloemendal (1970). Further studies on the ribonuclease inhibitor from rat liver: stability and other properties. *Biochim. Biophys. Acta* **224**, 55-62.

Haigis, M. C., E. S. Haag and R. T. Raines (2002). Evolution of ribonuclease inhibitor by exon duplication. *Mol. Biol. Evol.* **19**, 959-963.

Haigis, M. C., E. L. Kurten, R. L. Abel and R. T. Raines (2002). KFERQ sequence in ribonuclease A-mediated cytotoxicity. *J. Biol. Chem.* **277**, 11576-11581.

Haigis, M. C., E. L. Kurten and R. T. Raines (2002). Ribonuclease inhibitor is an intracellular sentry. *Nucleic Acids Res.* **31**, 1024-1032.

Haigis, M. C. and R. T. Raines (2003). Secretory ribonucleases are internalized by a dynamin-independent endocytic pathway. *J. Cell Sci.* **116**, 313-324.

Harper, J. W. and B. L. Vallee (1989). A covalent angiogenin/ribonuclease hybrid with a fourth disulfide bond generated by regional mutagenesis. *Biochemistry* **28**, 1875-1884.

Hofsteenge, J. (1997). Ribonuclease inhibitor. *Ribonucleases: Structures and Functions*. G. D'Alessio and J. F. Riordan. New York, Academic Press: 621-658.

Hofsteenge, J., B. Kieffer, R. Matthies, B. A. Hemmings and S. R. Stone (1988). Amino acid sequence of the ribonuclease inhibitor from porcine liver reveals the presence of leucine-rich repeats. *Biochemistry* **27**, 8537-8544.

Hofsteenge, J., A. Vicentini and O. Zelenko (1998). Ribonuclease 4, an evolutionarily highly conserved member of the superfamily. *Cell. Mol. Life Sci.* **54**, 804-810.

Hofsteenge, J., A. Vincentini and S. R. Stone (1991). Purification and characterization of truncated ribonuclease inhibitor. *Biochem. J.* **275**, 541-543.

Hu, G.-F., J. F. Riordan and B. L. Vallee (1997). A putative angiogenin receptor in angiogenin-responsive human endothelial cells. *Proc. Natl. Acad. Sci. USA* **94**, 2204-2209.

Jaffee, E. A., R. L. Nachman, C. G. Becker and C. R. Minick (1973). Culture of human endothelial cells derived from umbilical veins. Identification by morphologic and immunologic criteria. *J. Clin. Invest.* **52**, 2745-2756.

Janin, J. (1994). Proteins with a ring. *Structure* **2**, 571-573.

Jimi, S., K. Ito, K. Kohno, M. Ono, M. Kuwano, Y. Itagaki and H. Ishikawa (1995). Modulation by bovine angiogenin of tubular morphogenesis and expression of plasminogen activator in bovine endothelial cells. *Biochem. Biophys. Res. Commun.* **211**, 476-483.

Kajava, A. V. (1998). Structural diversity of leucine-rich repeat proteins. *J. Mol. Biol.* **277**, 519-527.

Kajava, A. V. and B. Kobe (2002). Assessment of the ability to model proteins with leucine-rich repeats in light of the latest structural information. *Prot. Sci.* **11**, 1082-1090.

Kawanomoto, M., K. Motojima, M. Sasaki, H. Hattori and S. Goto (1992). cDNA cloning and sequence of rat ribonuclease inhibitor, and tissue distribution of mRNA. *Biochim. Biophys. Acta* **1129**, 335-338.

Kelemen, B. R., T. A. Klink, M. A. Behlke, S. R. Eubanks, P. A. Leland and R. T. Raines (1999). Hypersensitive substrate for ribonucleases. *Nucleic Acids Res.* **27**, 3696-3701.

Kim, B.-M., L. W. Schultz and R. T. Raines (1999). Variants of ribonuclease inhibitor that resist oxidation. *Protein Sci.* **8**, 430-434.

Klink, T. A. and R. T. Raines (2000). Conformational stability is a determinant of ribonuclease A cytotoxicity. *J. Biol. Chem.* **275**, 17463-17467.

Klink, T. A., A. M. Vicentini, J. Hofsteenge and R. T. Raines (2001). High-level soluble production and characterization of porcine ribonuclease inhibitor. *Protein Exp. Purif.* **22**, 174-179.

Kobe, B. and J. Deisenhofer (1993). Crystal structure of porcine ribonuclease inhibitor, a protein with leucine-rich repeats. *Nature* **366**, 751-756.

Kobe, B. and J. Deisenhofer (1994). The leucine-rich repeat: A versatile binding motif. *Trends Biochem. Sci.* **19**, 415-421.

Kobe, B. and J. Deisenhofer (1995). Proteins with leucine-rich repeats. *Curr. Opin. Struct. Biol.* **5**, 409-416.

Kobe, B. and J. Deisenhofer (1995). A structural basis of the interactions βween leucine-rich repeats and protein ligands. *Nature* **374**, 183-186.

Kobe, B. and J. Deisenhofer (1996). Mechanism of ribonuclease inhibition by ribonuclease inhibitor protein based on the crystal structure of its complex with ribonuclease A. *J. Mol. Biol.* **264**, 1028-1043.

Kobe, K. and A. V. Kajava (2001). The leucine-rich repeat as a protein recognition motif. *Curr. Opin. Struct. Biol.* **11**, 725-732.

Kraft, N. and K. Shortman (1970). The phylogeny of the ribonuclease-ribonuclease inhibitor system: Its distribution in tissues and its response during leukaimogenesis and aging. *Aust. J. Biol. Sci.* **23**: 175-184.

Kraft, N., K. Shortman and D. Jamieson (1969). The effect of x-irradiation on the balance βween alkaline ribonuclease and the ribonuclease inhibitor of mammalian tissues. *Radiation Res.* **39**, 655-668.

Kumar, K., M. Brady and R. Shapiro (2004). Selective abolition of pancreatic RNase binding to its inhibitor protein. *Proc. Natl. Acad. Sci. USA* **101**, 53-58.

Kyner, D., J. K. Christman and G. Acs (1979). The effect of 12-*O*-tetradecanoyl-phorbol 13-acetate on the ribonuclease activity of circulating human lymphocytes. *Eur. J. Biochem.* **99**, 395-399.

Ledoux, L. (1955). Action of ribonuclease on certain ascites tumours. *Nature* **175**, 258-259.

Ledoux, L. (1955). Action of ribonuclease on two solid tumours *in vivo*. *Nature* **176**, 36-37.

Lee, F. S., D. S. Auld and B. L. Vallee (1989). Tryptophan fluorescence as a probe of placental ribonuclease inhibitor binding to angiogenin. *Biochemistry* **28**, 219-224.

Lee, F. S., E. A. Fox, H.-M. Zhou, D. J. Strydom and B. L. Vallee (1988). Primary structure of human placental ribonuclease inhibitor. *Biochemistry* **27**, 8545-8553.

Lee, F. S., R. Shapiro and B. L. Vallee (1989). Tight-binding inhibition of angiogenin and ribonuclease A by placental ribonuclease inhibitor. *Biochemistry* **28**, 225-230.

Lee, F. S. and B. L. Vallee (1989). Expression of human placental ribonuclease inhibitor in *Escherichia coli*. *Biochem. Biophys. Res. Commun.* **160**, 115-120.

Lee, F. S. and B. L. Vallee (1990). Modular mutagenesis of human placental ribonuclease inhibitor, a protein with leucine-rich repeats. *Proc. Natl. Acad. Sci. U.S.A.* **87**, 1879-1883.

Lee, F. S. and B. L. Vallee (1993). Structure and action of mammalian ribonuclease (angiogenin) inhibitor. *Prog. Nucleic Acid Res. Mol. Biol.* **44,** 1-30.

Leland, P. A. and R. T. Raines (2001). Cancer chemotherapy—ribonucleases to the rescue. *Chem. Biol.* **8**, 405-413.

Leland, P. A., L. W. Schultz, B.-M. Kim and R. T. Raines (1998). Ribonuclease A variants with potent cytotoxic activity. *Proc. Natl. Acad. Sci. U.S.A.* **98**, 10407-10412.

Leland, P. A., K. E. Staniszewski, B.-M. Kim and R. T. Raines (2000). A synapomorphic disulfide bond is critical for the conformational stability and cytotoxicity of an amphibian ribonuclease. *FEBS Lett.* **477**, 203-207.

Leland, P. A., K. E. Staniszewski, B. M. Kim and R. T. Raines (2001). Endowing human pancreatic ribonuclease with toxicity for cancer cells. *J. Biol. Chem.* **276**, 43095-43102.

Leland, P. A., K. E. Staniszewski, C. Park, B. R. Kelemen and R. T. Raines (2002). The ribonucleolytic activity of angiogenin. *Biochemistry* **41**, 1343-1350.

Makarov, A. A. and O. N. Ilinskaya (2003). Cytotoxic ribonucleases: Molecular weapons and their targets. *FEBS Lett.* **540**, 15-20.

Matousek, J. (1973). The effect of bovine seminal ribonuclease (AS RNase) on cells of crocker tumour in mice. *Experientia* **29**, 858-859.

Matousek, J., J. Soucek, J. Ríha, T. R. Zankel and S. A. Benner (1995). Immunosuppressive activity of angiogenin in comparison with bovine seminal ribonuclease and pancreatic ribonuclease. *Comp. Biochem. Physiol.* **112B**, 235-241.

Matousek, J. (1975). Embryotoxic effect of bull seminal ribonuclease and tissue absorption studies in rats. *J. Reprod. Fert.* **43**, 171-174.

Matousek, J. (1994). Aspermatogenic effect of the bull seminal ribonuclease (BS RNase) in the presence of anti BS RNase antibodies in mice. *Animal Genet.* **25**, 45-50.

Matousek, J. (2001). Ribonucleases and their antitumor activity. *Comp. Biochem. Physiol.* **129C**, 175-191.

Matousek, J., G. Gotte, P. Poucková, J. Sou_ek, T. Slavík, F. Vottariello and M. Libonati (2003). Antitumor activity and other biological actions of oligomers of ribonuclease A. *J. Biol. Chem.* **278**, 23817-23822.

Matteo, A. D., L. Federici, B. Mattei, G. Salvi, K. A. Johnson, C. Savino, G. D. Lorenzo and D. Tsernoglou (2003). The crystal structure of polygalacturonase-inhibiting protein (PGIP), a leucine-rich repeat protein involved in plant defense. *Proc. Natl. Acad. Sci. USA* **100**, 10124-10128.

Messmore, J. M., D. N. Fuchs and R. T. Raines (1995). Ribonuclease A: Revealing structure–function relationships with semisynthesis. *J. Am. Chem. Soc.* **117**, 8057-8060.

Mikulski, S. M., W. Ardelt, K. Shogen, E. H. Bernstein and H. Menduke (1990). Striking increase of survival of mice bearing M109 Madison carcinoma treated with a novel protein from amphibian embryos. *J. Natl. Cancer Inst.* **82**, 151-153.

Mikulski, S. M., H. G. Chung, A. Mittelman, T. Panella, C. A. Puccio, K. Shogen and J. J. Costanzi (1995). Relationship βween response rate and median survival in patients with advanced non-small cell lung cancer: Comparison of ONCONASE® with other anticancer agents. *Int. J. Oncol.* **6**, 889-897.

Mikulski, S. M., J. J. Costanzi, N. J. Vogelzang, S. McCachren, R. N. Taub, H. Chun, A. Mittelman, T. Panella, C. Puccio, R. Fine and K. Shogen (2002). Phase II trial of a single weekly intravenous dose of ranpirnase in patients with unresectable malignant mesothelioma. *J. Clin. Oncol.* **20**, 274-281.

Mikulski, S. M., A. M. Grossman, P. W. Carter, K. Shogen and J. J. Costanzi (1993). Phase I human clinical trial of ONCONASE (P-30 Protein) administered intravenously on a weekly schedule in cancer patients with solid tumors. *Int. J. Oncol.* **3**, 57-64.

Moenner, M., M. Gusse, E. Hatzi and J. Badet (1994). The widespread expression of angiogenin in different human cells suggests a biological function not only related to angiogenesis. *Eur. J. Biochem.* **226**, 483-490.

Moenner, M., M. Vosoghi, S. Ryazantsev and D. G. Glitz (1998). Ribonuclease Inhibitor protien of human erythrocytes: Characterization, loss of activity in response to oxidative stress, and association with Heinz bodies. *Blood Cells, Molecules, and Diseases* **24**, 149-164.

Monti, D. M. and G. D'Alessio (2004). Cytosolic RNase inhibitor only affects RNases with intrinsic cytotoxicity. *J. Biol. Chem.* **279**, 39195-39198.

Moore, S. and W. H. Stein (1973). Chemical structures of pancreatic ribonuclease and deoxyribonuclease. *Science* **180**, 458-464.

Moroianu, J. and J. F. Riordan (1994). Identification of the nucleolar targeting signal of human angiogenin. *Biochem. Biophys. Res. Commun.* **203**, 1765-1772.

Moroianu, J. and J. F. Riordan (1994). Nuclear translocation of angiogenin in proliferating endothelial cells is essential to its angiogenic activity. *Proc. Natl. Acad. Sci. U.S.A.* **91**, 1677-1681.

Mosimann, S. C., W. Ardelt and M. N. G. James (1994). Refined 1.7 Å X-ray crystallographic structure of P-30 protein, an amphibian ribonuclease with anti-tumor activity. *J. Mol. Biol.* **236**, 1141-1153.

Nadano, D., T. Yasuda, H. Takeshita, K. Uchide and K. Kishi (1994). Purification and characterization of human brain ribonuclease inhibitor. *Arch. Biochem. Biophys.* **312**, 421-428.

Newton, D. L., L. Boque, A. Wlodawer, C. Y. Huang and S. M. Rybak (1998). Single amino acid substitutions at the N-terminus of a recombinant cytotoxic ribonuclease markedly influence biochemical and biological properties. *Biochemistry* **37**, 5173-5183.

Newton, D. L., Y. Xue, L. Boque, A. Wlodawer, H. F. Kung and S. M. Rybak (1997). Expression and characterization of a cytotoxic human-frog chimeric ribonuclease: Potential for cancer therapy. *Protein Eng.* **10**,463-470.

Nitta, K., K. Ozaki, M. Ishikawa, S. Furusawa, M. Hosono, H. Kawauchi, K. Sasaki, Y. Takayanagi, S. Tsuiki and S. Hakomori (1994). Inhibition of cell proliferation by *Rana catesbeiana* and *Rana japonica* lectins belonging to the ribonuclease superfamily. *Cancer Res.* **54**, 920-927.

Nitta, K., G. Takayanagi, H. Kawauchi and S. Hakomori (1987). Isolation and characterization of Rana catesbeiana lectin and demonstration of the lectin-binding glycoprotein of rodent and human tumor cell membranes. *Cancer Res.* **47**, 4877-4883.

Olson, K. A., H. R. Byers, M. E. Key and J. W. Fett (2002). Inhibition of prostate carcinoma establishment and metastatic growth in mice by an antiangiogenin monoclonal antibody. *Int. J. Cancer* **98**, 923-929.

Olson, K. A., J. R. Byers, M. E. Key and J. W. Fett (2001). Prevention of human prostate tumor metastasis in athymic mice by antisense targeting of human angiogenin. *Clin. Cancer Res.* **7**, 3598-3606.

Papageorgiou, A., R. Shapiro and K. Acharya (1997). Molecular recognition of human angiogenin by placental ribonuclease inhibitor—an X-ray crystallographic study at 2.0 Å resolution. *EMBO J.* **16**, 5162-5177.

Pasloske, B. L. (2001). Ribonuclease inhibitors. *Nuclease Methods and Protocols*. C. H. Schein. Totowa, NJ, Humana Press: 105 - 111.

Pavlov, N. and J. Badet (2001). Angiogenin: Involvement in angiogenisis and tumor growth. *Bull. Cancer* **88**, 725-732.

Pirotte, M. and V. Desreux (1952). *Bull. Soc. Chim. Belg.* **61**, 167.

Polakowski, I. J., M. K. Lewis, V. Muthukkaruppan, B. Erdman, L. Kubai and R. Auerbach (1993). A ribonuclease inhibitor expresses anti-angiogenic properties and leads to reduced tumor growth in mice. *Am. J. Pathol.* **143**, 507-517.

Price, S. R., P. R. Evans and K. Nagai (1998). Crystal structure of the spliceosomal U2B"-U2A' protein complex bound to a fragment of U2 small nuclear RNA. *Nature* **394**, 645-650.

Raines, R. T. (1998). Ribonuclease A. *Chem. Rev.* **98**, 1045-1065.

Raines, R. T. (1999). Ribonuclease A: from model system to cancer chemotherapeutic. *Enzymatic Mechanisms*. P. A. Frey and D. B. Northrop. Washington, DC, IOS Press: 235-249.

Ribó, M., E. Fernández, J. Bravo, M. Osset, M. J. M. Fallon, R. de Llorens and C. M. Cuchillo (1991). Purification of human pancreatic ribonuclease by high performance liquid chromatography. *Structure, Mechanism and Function of Ribonucleases*. R. de Llorens, C. M. Cuchillo, M. V. Nogués and X. Parés. Bellaterra, Spain, Universitat Autónoma de Barcelona: 157-162.

Riordan, J. F. (2001). Angiogenin. *Methods Enzymol.* **341**, 263-273.

Roth, J. S. (1962). Ribonuclease IX. Further studies on ribonuclease inhibitor. *Biochim. Biophys. Acta* **61**, 903-915.

Roth, J. S. (1963). Ribonuclease activity and cancer: A review. *Cancer Res.* **23**, 657-666.

Roth, J. S. (1967). Some observations on the assay and properties of ribonucleases in normal and tumor tissues. *Methods Cancer Res.* **3**, 153-242.

Rutkoski, T. J., E. L. Kurten, J. C. Mitchell and R. T. Raines (2005). Disruption of shape-complementarity markers to create cytotoxic variants of ribonuclease A. *J. Mol. Biol.* **354**, 41-54.

Scacheri, P. C., O. Rozenblatt-Rosen, N. J. Caplen, T. G. Wolfsberg, L. Umayam, J. C. Lee, C. M. Hughes, K. S. Shanmugam, A. Bhattecharjee, M. Meyerson and F. S. Collins (2003). Short interfering RNAs can induce unexpected and divergent changes in the levels of untargeted proteins in mammalian cells. *Proc. Natl. Acad. Sci. U.S.A.* **101**,1892-1897.

Schneider, R., E. Schneider-Scherzer, M. Thurnher, B. Auer and M. Schweiger (1988). The primary structure of human ribonuclease/angiogenin inhibitor (RAI) discloses a novel highly diversified protein superfamily witha common repetitive module. *EMBO J.* **7**, 4151-4156.

Schott, P. G., P. A. McEwan, C. M. Dodd, E. M. Bergmann, P. N. Bishop and J. Bella (2004). Crystal structure of the dimeric protein core of decorin, the archetypal small leucine-rich repeat proteoglycan. *Proc. Natl. Acad. Sci. U S A* **101**, 15633-15638.

Schulman, B. A., A. C. Carrano, P. D. Jeffrey, Z. Bowen, E. R. E. Kinnucan, M. S. Finnin, S. J. Elledge, J. W. Harper, M. Pagano and N. P. Pavletich (2000). Insights into SCF ubiquitin ligases from the structure of the Skp1-Skp2 complex. *Nature* **408**, 381-386.

Sela, M., C. B. Anfinsen and W. F. Harrington (1957). The correlation of ribonuclease activity with specific aspects of tertiary structure. *Biochim. Biophys. Acta* **26**, 502-512.

Shapiro, R. (2001). Cytoplasmic ribonuclease inhibitor. *Methods Enzymol.* **341**, 611-628.

Shapiro, R., E. A. Fox and J. F. Riordan (1989). Role of lysines in human angiogenin: chemical modification and site-directed mutagenesis. *Biochemistry* **28**, 1726-1732.

Shapiro, R. and J. F. Riordan (1989). Site-directed mutagenesis of histidine-13 and histidine-114 of human angiogenin. Alanine derivatives inhibit angiogenin-induced angiogenesis. *Biochemistry* **28**, 7401-7408.

Shapiro, R., J. F. Riordan and B. L. Vallee (1995). LRRning the RIte of springs. *Nat. Struct. Biol.* **2**, 350-354.

Shapiro, R., M. Ruiz-Gutierrez and C. Z. Chen (2000). Analysis of the interactions of human ribonuclease inhibitor with angiogenin and ribonuclease A by mutagenesis: Importance of inhibitor residues inside versus outside the C-terminal "hot spot". *J. Mol. Biol.* **302**, 497-519.

Shapiro, R. and B. L. Vallee (1987). Human placental ribonuclease inhibitor abolishes both angiogenic and ribonucleolytic activities of angiogenin. *Proc. Natl. Acad. Sci. U.S.A.* **84**, 2238-2241.

Shapiro, R. and B. L. Vallee (1991). Interaction of human placental ribonuclease with placental ribonuclese inhibitor. *Biochemistry* **30**, 2246-2255.

Slavík, T., J. Matou_ek, J. Fulka and R. T. Raines (2000). Effect of bovine seminal ribonuclease and bovine pancreatic ribonuclease A on bovine oocyte maturation. *J. Exp. Zool.* **287**, 394-399.

Strydom, D. J. (1998). The angiogenins. *Cell. Mol. Life Sci.* **54**, 811-824.

Stumpp, M. T., P. Forrer, H. K. Binz and A. Pluckthun (2003). Designing repeat protiens: Modular leucine-rich repeat protein libraries based on mammalian ribonuclease inhibitor family. *J. Mol. Bio.* **332**, 471-487.

Suzuki, Y. and Y. Takahashi (1970). Developmental and regional variations in ribonuclease inhibitor activity in brain. *J. Neurochem.* **17**, 1521-1524.

Takahashi, N., Y. Takahashi and F. W. Putnam (1985). Periodicity of leucine and tandem repetition of a 24-amino acid segment in the primary structure of leucine-rich αha 2-glycoprotein of human serum. *Proc. Natl. Acad. Sci. USA* **82**, 1906-1910.

Tanford, C. and J. D. Hauenstein (1956). Hydrogen Ion Equilibria of Ribonuclease. *J. Am. Chem. Soc.* **78**, 5287-5291.

Teufel, D. P., R. Y. T. Kao, K. R. Acharya and R. Shapiro (2003). Mutational analysis of the complex of human RNase inhibitor and human eosinophil-derived neurotoxin. *Biochemistry* **42**, 1451-1459.

Vasandani, V. M., Y.-N. Wu, S. M. Mikulski, R. J. Youle and C. Sung (1996). Molecular determinants in the plasma clearance and tissue distribution of ribonucleases of the ribonuclease A superfamily. *Cancer Res.* **56,** 4180-4186.

Vescia, S., D. Tramontano, G. Augusti-Tocco and G. D'Alessio (1980). *In vitro* studies on selective inhibition of tumor cell growth by seminal ribonuclease. *Cancer Res.* **40**, 3740-3744.

Vicentini, A. M., B. Kieffer, R. Mathies, B. Meyhack, B. A. Hemmings, S. R. Stone and J. Hofsteenge (1990). Protein chemical and kinetic characterization of recombinant porcine ribonuclease inhibitor expressed in *Saccharomyces cerevisiae*. *Biochemistry* **29,** 8827-8834.

Wlodawer, A. (1985). Structure of bovine pancreatic ribonuclease by X-ray and neutron diffraction. *Biological Macromolecules and Assemblies, Vol. II, Nucleic Acids and Interactive Proteins*. F. A. Jurnak and A. McPherson. New York, Wiley: 395-439.

Wojnar, R. J. and J. S. Roth (1965). Ribonuclease inhibitor and latent ribonuclease in rat liver during feeding of 2-acetamidofluorene. *Cancer Res.* **25**, 1913-1918.

Wu, Y., S. M. Mikulski, W. Ardelt, S. M. Rybak and R. J. Youle (1993). A cytotoxic ribonuclease. *J. Biol. Chem.* **268,** 10686-10693.

Xu, Z.-p., T. Tsuji, J. F. Riordan and G.-F. Hu (2003). Identification and characterization of an angiogenin-binding DNA sequence that stimulates luciferase reporter gene expression. *Biochemistry* **42**, 121-128.

Xu, Z. P., T. Tsuji, J. F. Riordan and G. F. Hu (2002). The nuclear function of angiogenin in endothelial cells is related to rRNA production. *Biophys. Res. Commun.* **294**, 287-292.

Youle, R. J. and G. D'Alessio (1997). Antitumor RNases. *Ribonucleases: Structures and Functions*. G. D'Alessio and J. F. Riordan. New York, Academic Press: 491-514.

Zelenko, O., U. Neumann, W. Brill, U. Pieles, H. E. Moser and J. Hofsteenge (1994). A novel fluorogenic substrate for ribonucleases. Synthesis and enzymatic characterization. *Nucleic Acids Res.* ***22,*** 2731-2739.

Zhang, J., K. D. Dyer and H. F. Rosenberg (2003). Human RNase 7: a new cationic ribonuclease of the RNase A superfamily. *Nucleic Acids Res* **31**, 602-607.

Zimmerman, S. B. and A. P. Minton (1991). Estimation of macromolecule concentrations and excluded volume effects for the cytoplasm of *Escerichia coli*. *J. Mol. Biol.* **222**, 599-620.